Copyright Warning & Restrictions

The copyright law of the United States (Title 17, United States Code) governs the making of photocopies or other reproductions of copyrighted material.

Under certain conditions specified in the law, libraries and archives are authorized to furnish a photocopy or other reproduction. One of these specified conditions is that the photocopy or reproduction is not to be "used for any purpose other than private study, scholarship, or research." If a, user makes a request for, or later uses, a photocopy or reproduction for purposes in excess of "fair use" that user may be liable for copyright infringement,

This institution reserves the right to refuse to accept a copying order if, in its judgment, fulfillment of the order would involve violation of copyright law.

Please Note: The author retains the copyright while the New Jersey Institute of Technology reserves the right to distribute this thesis or dissertation

Printing note: If you do not wish to print this page, then select "Pages from: first page # to: last page #" on the print dialog screen

ABSTRACT

SURFACE RECORDINGS OF EVOKED FIELD POTENTIALS FROM THE CEREBELLUM WITH A FLEXMEA MICROELECTRODE ARRAY

by
Jonathan David Groth

The cerebellum is an integral part of multijoint control. There are two input pathways to the cerebellar cortex, the mossy fiber and the climbing fiber pathways. The mossy fiber pathway forms a disynaptic input to Purkinje cells through the granular cells. This disynaptic input produces a multicomponent field potential composed of the P1, N1, N2, N3, N4, and P3 waves. The climbing fiber input forms a monosynaptic input to the Purkinje cells and thus creates a much simpler field potential.

The mossy and climbing fiber field potentials were recorded with a FlexMEA microelectrode array from the pial surface of the paramedian lobule. The peripheral stimulation showed that the mossy and climbing fiber field potentials evoked through intramuscular stimulation were consistent with those of the literature. These results verified the experimental setup to be used in the central stimulation.

The central stimulation produced only the mossy fiber field potential. The amplitude of the field potentials were mapped out to the location on the electrode array producing unique maps for each stimulation site. ANOVA analysis showed that distinct regions can be associated with a certain region of stimulation.

These results show that the FlexMEA is able to record the field potentials from the pial surface of the cerebellar cortex. The 300μm pitch of the electrodes in the array produces distinct patterns with clear regions of activity for different sites of stimulation. In conclusion the FlexMEA can be used to record from cerebellum in behaving animals.

SURFACE RECORDINGS OF EVOKED FIELD POTENTIALS FROM THE CEREBELLUM WITH A FLEXMEA MICROELECTRODE ARRAY

by
Jonathan David Groth

A Thesis
Submitted to the Faculty of
New Jersey Institute of Technology
in Partial Fulfillment of the Requirements for the Degree of
Master of Science in Biomedical Engineering

Department of Biomedical Engineering

May 2008

APPROVAL PAGE

SURFACE RECORDINGS OF EVOKED FIELD POTENTIALS FROM THE CEREBELLUM WITH A FLEXMEA MICROELECTRODE ARRAY

Jonathan David Groth

Dr. Mesut Sahin, Thesis Advisor — Date
Assistant Professor of Biomedical Engineering, NJIT

Dr. Tara Alvarez, Committee Member — Date
Associate Professor of Biomedical Engineering, NJIT

Dr. Bryan Pfister, Committee Member — Date
Assistant Professor of Biomedical Engineering, NJIT

BIOGRAPHICAL SKETCH

Author: Jonathan David Groth

Degree: Master of Science

Date: May 2008

Undergraduate and Graduate Education:

- Masters of Science in Biomedical Engineering,
  New Jersey Institute of Technology, Newark, NJ, 2008

- Bachelors of Science in Biomedical Engineering,
  Louisiana Tech University, Ruston, Louisiana, 2005

Major: Biomedical Engineering

Presentations and Publications:

Groth, J., Sahin, M., "Cerebellar Surface Recordings with a FlexMea Electrode" Northeast Bioengineering Conference Proceedings, 2008.

To my parents who raised be with both a love of science and of God
without either I could not be here now.

ACKNOWLEDGMENT

I would like to thank my advisor Dr. Mesut Sahin For his help and guidance through out this project and for his willingness to answer all kinds of questions give long hours in the lab to get this project done. I would like to also thank Dr. Tara Alvarez for her neural engineering class which was invaluable in my project and her support as a member of my committee and our discussion and her pointers on the project. I would also like to thank Dr. Bryan Pfister for his help on my presentation and in our discussion on the project.

TABLE OF CONTENTS

TABLE OF CONTENTS
(Continued)

LIST OF FIGURES

LIST OF FIGURES
(Continued)

Figure **Page**

LIST OF FIGURES
(Continued)

Figure **Page**

LIST OF FIGURES
(Continued)

Figure **Page**

LIST OF FIGURES
(Continued)

Figure **Page**

LIST OF FIGURES
(Continued)

Figure **Page**

CHAPTER 1

INTRODUCTION

1.1 Objective

The cerebellum is an important component in movement control. There is still much to learn about the processing and control of movement parameters in the cerebellum. The objective of this thesis was to demonstrate the feasibility of using the FlexMea micro-electrode array to record field potentials from the pial surface of the rat cerebellar cortex.

The cerebellum signals were recorded from the paramedian lobule with the Flex Mea micro-electrode array. The FlexMea array has 32 recording contacts with an interelectrode distance of 300μm. Two types of stimulation were used. The first stimulation used was peripheral stimulation which was achieved through intramuscular stimulation. The second form of stimulation used was the stimulation of the primary motor cortex.

This report will describe the field potentials from paramedian lobule of the cerebellum evoked by both peripheral stimulation and stimulation of the primary motor cortex. 1) The field potentials of the cerebellum evoked by the peripheral stimulation will be compared to that of previous published works. 2) The central stimulation evoked potentials will be compared to that of the peripherally evoked potentials. 3) The amplitudes of the centrally evoked potentials will be mapped out to the position of the electrodes on the FlexMea array to show the area of activation for different stimulation sites. 4) The statistical method of ANOVA will be used to determine the selectivity of the electrodes to a site of activity.

1.2 Background Information

The cerebellum is involved in the coordination of movement. The cerebellum receives information from the spinal cord and the cerebral cortex and other nuclei. The cerebellum then sends information back out to the cerebral cortex via the thalamus and to the rubro-spinal tract. This loop with the motor and pre-motor cortex, the basal ganglia, spinal cord, and the cerebellum forms the central motor system.

1.2.1 Anatomy of the Cerebellar Cortex

The primary processing of the cerebellum takes place in the cerebellar cortex. The cerebellar cortex consists of 3 layers listed here from deep to superficial: Granular layer, Purkinje layer, and the molecular layer. The primary processing element of the cerebellum is the Purkinje cell that receives input from the climbing fiber tract and the mossy-granular-parallel fiber tract. The climbing fiber forms a monosynaptic input to the Purkinje fiber and the mossy fiber forms a dysynaptic input synapsing on the granular cells which then synapse on the Purkinje fibers. Figure 1 shows both the climbing fiber and mossy-granular-parallel fiber tracts in orientation to the Purkinje fibers [1].

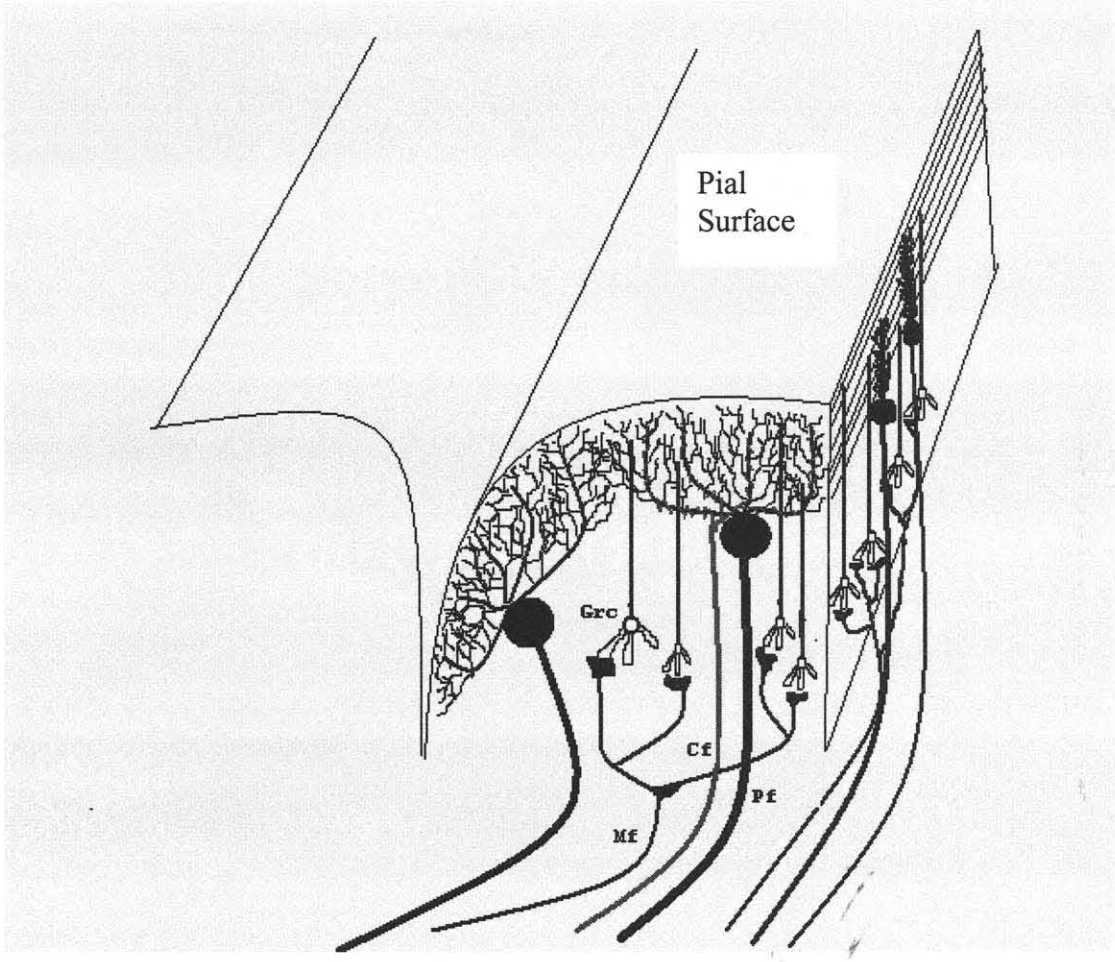

Figure 1.1 The cerebellar cortex with the Purkinje fibers (**Pf**), mossy fibers (**Mf**), granular cells (**Grc**), and climbing fibers (**Cf**).

The human Purkinje fiber can form up to 200,000 synapses. This is a result of its large dendritic tree that expands out into a single plane intersecting the large number of parallel fibers that run perpendicular to the plane of the Purkinje fiber in the molecular layer. The soma in the Purkinje layer is spherical in shape with a slender axon that extends down through the granular region to the cerebellar nuclei [1].

The climbing fibers rises from the inferior olive where they receive inputs from the spinal cord, brainstem, cerebellar nuclei, and cerebral cortex. The climbing fiber enters the cerebellum through the inferior peduncle. The climbing fiber then synapse on

the deep cerebellar nuclei. It then raises though the cerebellum and branches off into several collaterals. Rising up to the molecular layer, it climbs up the Purkinje fiber wrapping around the dendrites and forming synapses along the way. A single Purkinje fiber is innervated by only a single climbing fiber, however, a single climbing fiber can innervate several Purkinje fibers [1].

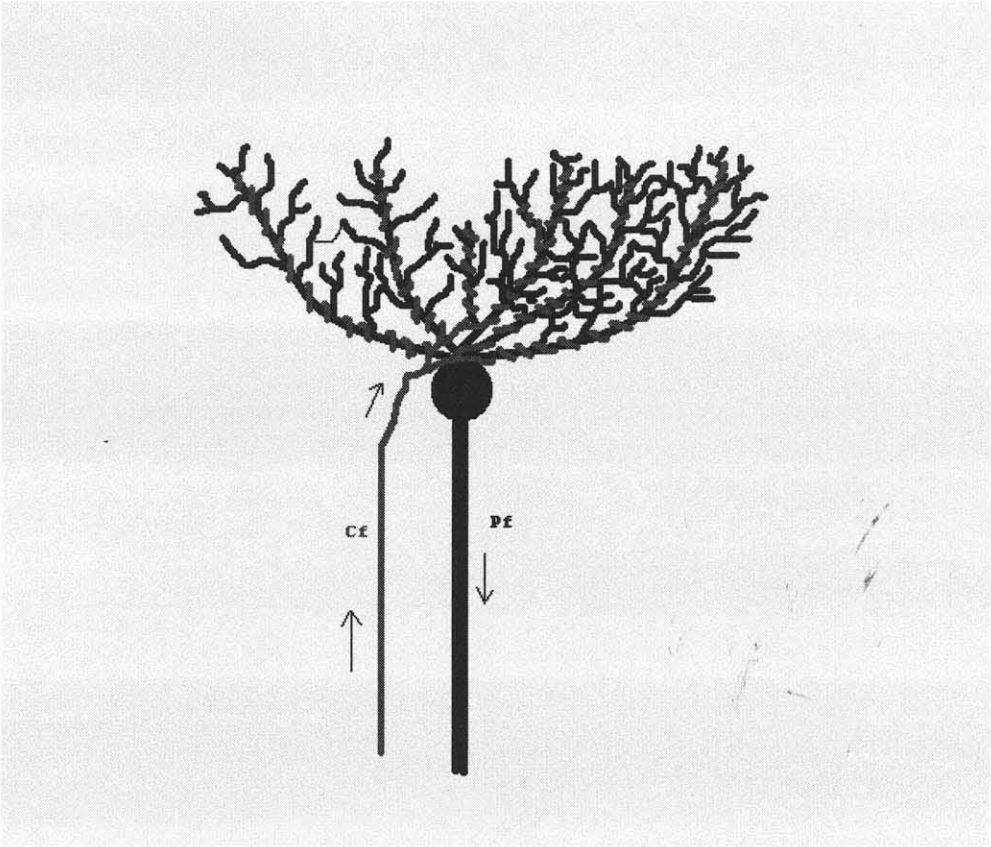

Figure 1.2 The climbing fiber (**Cf**) rises up and wraps around the Purkinje fiber (**Pf**) dendritic tree forming many synapses as it climbs. The arrows show the travel direction of the impulses along the individual axons.

The mossy fibers arise from many regions in the brain among these are the spinal cord and the pontine nuclei. The pontine nuclei receive input from the cerebral cortex, which include the motor and pre-motor cortex. The mossy fibers enter the cerebellum through the inferior, middle, and superior peduncles. They then rise, branching on the

way so that they innervate several folia of the cerebellum, to the granular layer where they synapse on to the granular cells; the granular cells are the most numerous neurons in the central nervous system shown in Figure 1.3. The granular cells then rise up to the molecular layer where they bifurcate into two fibers that run in opposite directions. These fibers run in parallel with the other bifurcating granular fibers thus they are named parallel fibers. These parallel fibers run in a direction that is perpendicular to the plane of Purkinje dendritic arborations. The parallel fibers form both direct synapses and enpasant synapses with the Purkinje fibers. A single parallel fiber's EPSP on the Purkinje fiber is insufficient to create an action potential and thus it takes many parallel fibers acting on the Purkinje fiber to produce a potential strong enough create an impulse. The parallel fibers also synapse with all of the inhibitory neurons of the cerebellar cortex [1].

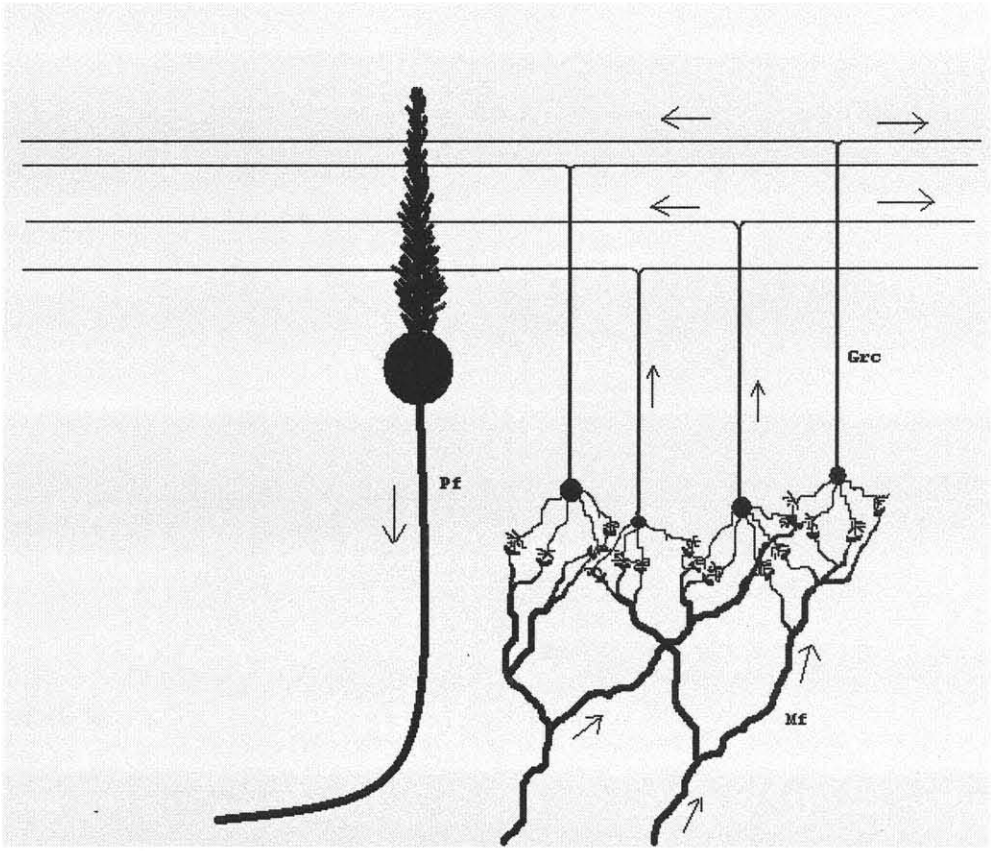

Figure 1.3 This diagram shows mossy-granular-parallel fiber tract with the mossy fibers (**Mf**), granular cells (**Grc**), and Purkinje fibers (**Pf**). The arrows show the direction of travel of the impulses along the individual axons.

There are three inhibitory neurons in the cerebellar cortex: Golgi cells, basket cells, and stellate cells. The inhibitory neurons are shown in Figure 1.4 in conjunction with the mossy-granular-parallel fiber pathway. The Golgi cells are found in the granular layer where they synapse onto the granular cell dendrites. The Golgi cells receive their input from the parallel fibers in the molecular layer and the mossy and climbing fibers in the granular layer. The basket cells are found in the lower regions of the molecular layer. The stellate cells are found in the middle and upper regions of the molecular layer. Both the basket and stellate cells receive their input from the parallel fibers synapse on the Purkinje fibers [1].

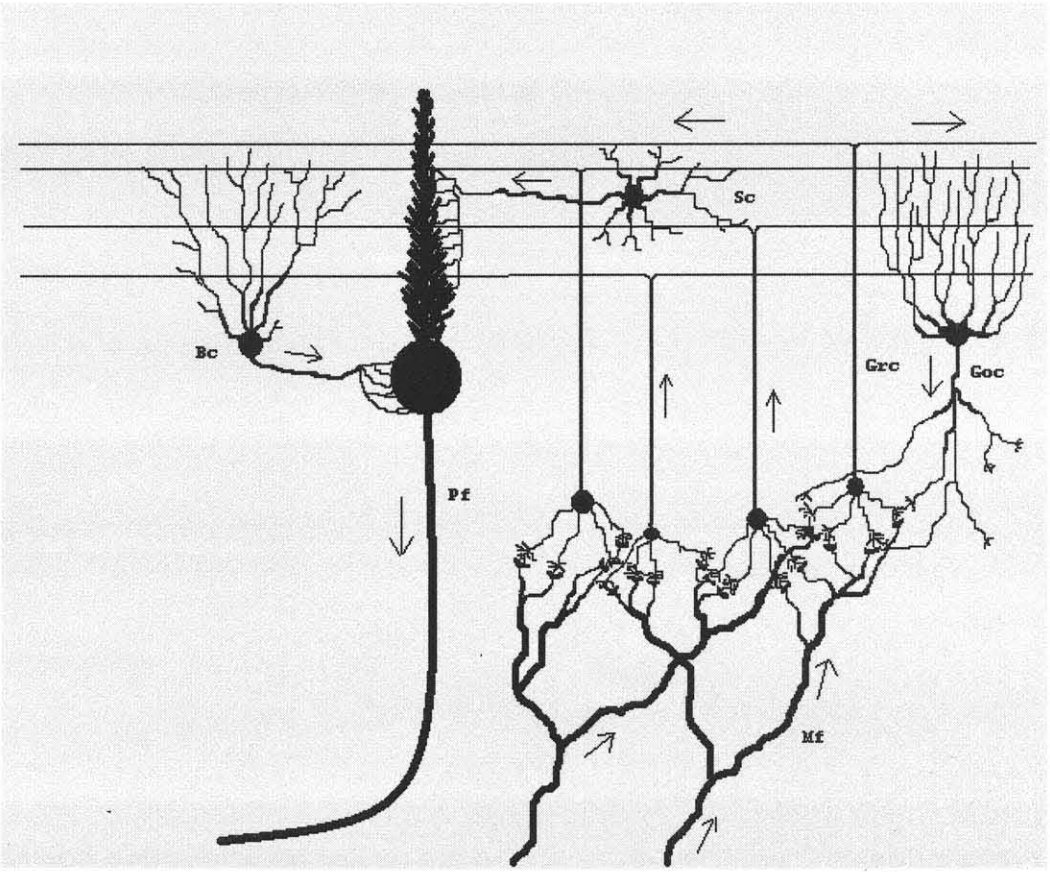

Figure 1.4 The mossy-granular-parallel fiber system, Purkinje cells (**Pf**), mossy fibers (**Mf**), granular cells (**Grc**), with inhibitory neurons, basket cells (**Bc**), stellate cells (**Sc**), and Golgi cells (**Goc**).

1.2.2 Function of the Cerebellum

The exact function of the cerebellum is still being debated. There are a number of theorems that are proposed, however none of them have a large enough body of evidence to support them. To understand the cerebellum it is important to understand the connections of the cerebellum to other areas of the central nervous system and the type of information that is being processed.

In a study of the dorsal spinocerebellar tract in cats, Bosco et al [2] showed that signals leading to the cerebellum were modulated by both position and movement. They found that 31.6% of the cells recorded were modulated by position alone and that 58.2%

of the cells were modulated by movement and position. The movement related signal of the movement and position modulated cells was affected by the position of the limb in a multiplicative fashion. They also found that these cells showed a tendency for a preferred direction in the direction of the limb axis or perpendicular to it. They concluded that the dorsal spinocerebellar neurons operate as a limb oriented coordinate system .

Since the information entering the cerebellum is modulated by multiple signals it is not surprising that the cerebellar Purkinje cells are also modulated by multiple parameters of the limb. The first to be explored was the position sensitivity of the Purkinje fibers. Like the motor cortex, the Purkinje cells were found to be modulated by the position of the limb. They were also found to follow the same cosine model fit like the cells of the motor and premotor areas as shown in figure 1.5. However, unlike the neurons of the motor and premotor cortex, the Purkinje cells did not show a uniform distribution of preferred direction rather they showed predominance in the parasagittal plane of movement [3, 4, 5].

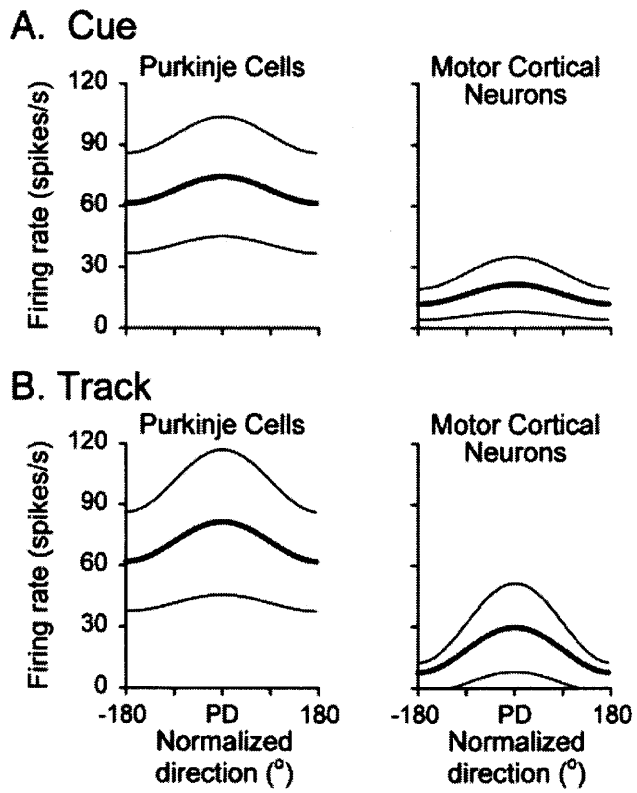

Figure 1.5 The cosine models for the Purkinje cells and motor cortical neurons showing that both regions show a cosine model fit with a preferred direction. [Johnson, M. T. V., and Ebner, T. J., "Processing of multiple kinematic signals in the cerebellum and motor cortices," *Brain Research Reviews*, vol. 33, pp. 155-168, 2000.]

.

Direction related modulation related to only a small percentage of the total possible modulation of the cell which could allow for multiple signals to be represented [3, 4, 5]. Distance and Speed were also shown to modulate the Purkinje cell discharge [4, 5, 6]. Many cells in the cerebellum were modulated by both speed and direction [4, 5, 6]. These cells showed a direction modulation at only one speed or distance or a speed or distance modulation at only one direction [4, 5]. It has been proposed that the Purkinje fibers may represent the velocity of the limb [4, 5, 6].

In the neurons of the motor cortex, that represent two different motor parameters, the different signals are represented in temporally distinct sequences, with the direction modulation coming first and the distance and speed modulation coming second. In the cerebellum, the Purkinje cells are modulated at the same time for all types of movement parameters [4, 5]. Ebner concluded that this was due to the real time control of movement that takes place in the cerebellum [4].

Several models have been proposed on how the cerebellum processes the information and how the brain uses its output. Kawato and Gomi proposed a feedback-error-learning scheme were the climbing fibers represent an error signal [7]. Kettner et al proposed a predictive control model for the cerebellar control of smooth eye pursuits [8]. Hirano proposed the cerebellum is involved in feed-forward associative learning [9]. Recently these two models have been combined with the idea of the cerebellum as a place for internal model creation. There are two forms of internal models that are being looked into, the inverse model [10, 11] and the forward model [10, 12]. The inverse model would use sensory information about the limbs kinematics and develop the appropriate motor signal to compare versus the actual motor signal [13]. The forward model use efferent copies of motor commands and predict sensory consequences [13].

1.2.3 Functional Organization

The cerebellum has four major functional regions. The vermis is the central portion of the cerebellum and is involved in balance. The area immediately lateral to the vermis is the paravermis, also called the spinocerebellum, which is involved in control of movement and error correction. The most lateral regions of the cerebellum contribute to motor planning [14].

There are two somatotopic maps in the spinocerebellar region one on the anterior and one on the posterior faces [14]. However the somatotopic maps are not composed of continuous areas representing a certain region of the body rather they are composed of a mosaic of patches called fractured somatotopy [15]. This means that the regions for a particular body region are represented on the cerebellar cortex by several small patches for particular parts of a region broken up by patches for other regions for example the forearm and paw are broken up by regions of the face and jaw on the paramedian lobule[15]. The climbing fibers form the basic organization for these regions [16]. The mossy fibers and climbing fibers for the same region of the body rise to the same areas in the cerebellar cortex [17]. However the mossy fibers form slightly larger patches than do the climbing fibers [17].

1.2.4 Signal Nature and Components

The field potentials for the mossy fiber volleys were first detailed by Eccles et al. in 1967 [18]. They studied the mossy fiber volleys by juxta-fastigial stimulation, stimulation of the deep white matter of the cerebellum, and trans-folial stimulation, stimulation of an adjacent folium's molecular layer. They recorded the field potential using a micro electrode at varying depths in the cerebellar cortex. This allowed them to determine the region and thus the structures that gave rise to the individual components.

The results showed that the components of the field potentials arise from distinct regions of the cortex. The P1/N1 wave had the normal form of an impulse traveling up a nerve and thus arises from the propagation of the action potentials up the mossy fiber axons. The N2 was strongest in the granular layer and had the form of a slow excitatory post synaptic potential (EPSP). They determined that it was due to the excitation of the granule and Golgi cells. The P2/N3 wave arose simultaneously from the transmission of the impulse up the granular cells and the excitation of the Purkinje cells. The P2 wave was detected while recording in the granular layer and lower and the N3 wave was detected in the molecular layer. The N4 wave was the result of the impulse traveling down the Purkinje axon. The P3 wave was believed to be produced by the IPSP of the inhibitory neurons in the cerebellar cortex [18]. Figure 1.6 shows a graphical representation of the origin of the mossy fiber field potential and Figure 1.7 shows the results of Eccles experiments showing the mossy fiber potentials at varying depths.

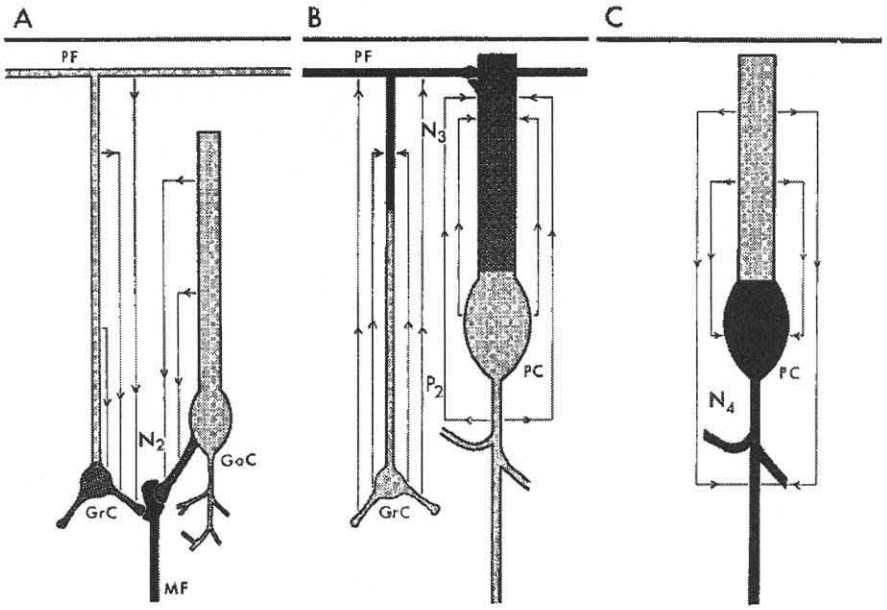

Figure1.6 graphical representation of the origin of the potential fields. The N1 wave, not shown, arises from the impulse traveling along the mossy fiber. The N2 wave arises from the EPSP on the granular cells and Golgi cells. The P2/N3 wave arises from the Impulses traveling up the granular cell axon and the EPSP of the Parallel fibers on the Purkinje cells. The N4 wave arises from the impulse traveling down the Purkinje fiber. [Eccles, J. C., Sasaki, K., Strata, P., "Interpretation of the potential fields generated in the cerebellar cortex by a mossy fiber volley," Experimental Brain Research, vol. 3, pp. 58-80, 1967]

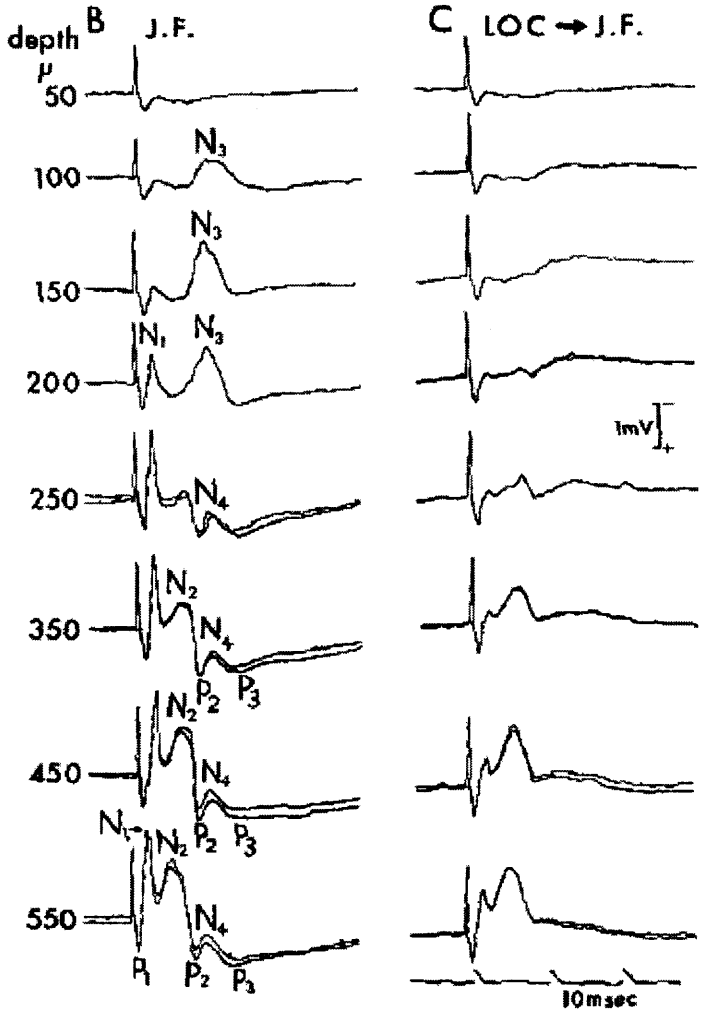

Figure 1.7 The results of Eccles et al experiments showing the mossy fiber field potential at varying depths. The P1, N1, N2, N2, P2, N4, and P3 waves are marked for each depth. [Eccles, J. C., Sasaki, K., Strata, P., "Interpretation of the potential fields generated in the cerebellar cortex by a mossy fiber volley," Experimental Brain Research, vol. 3, pp. 58-80, 1967]

Armstrong et al. [19] performed a similar experiment though they stimulated the cutaneous afferent fibers and recorded on the pial surface. They showed that the surface recordings were the similar to those recorded in the molecular layer. They also showed that the N1 peak occurred at a latency of approximately 2.4ms. The N1 peak was followed by the N2 peak and N3 peak. The N3 peak occurred at a latency of 5.0ms. The results of their experiments are shown in Figure 1.8.

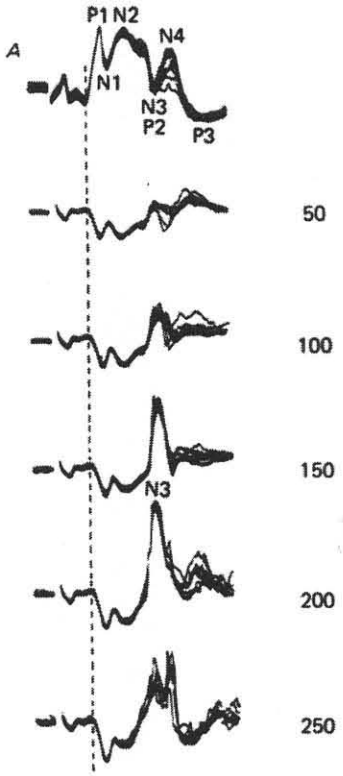

Figure 1.8 The results of the Armstrong et al. experiments showing the mossy fiber field potentials, evoked by stimulation of the cutaneous afferents, at varying depths. The top plot represents the surface field potential and the components are marked. [Armstrong, D. M., Drew, T., "Responses in the posterior lobe of the rat cerebellum to electrical stimulation of cutaneous afferents to the snout," Journal of Physiology, vol. 309, pp. 357-374, 1980.].

CHAPTER 2

MATERIALS AND METHODS

2.1 Animal Subject

The experiments were performed on Sprague-Dawley rats from Charles's River. The weights of the rats ranged from 300 to 550g. Successful peripheral stimulation was achieved in one rat. Successful central stimulation was achieved in one rat. All anesthetic, surgical, and experimental procedures were approved by the Rutgers Animal Welfare Committee.

2.2 Surgical Procedure

The rat was anesthetized with 80mg/kg ketamine and 12mg/kg xylazine injected intraperitonia. Anesthesia was maintained by injecting 20mg/kg ketamine every 20 minutes. In order to insert the tracheal tube a cut was made, through the skin, 2.5 cm down the mid line of the rat's neck from the sternum. A pair of sharp scissors was used to separate the muscle that lies over the trachea. The trachea was lifted up with the scissors avoiding the nerves and tissue behind it. After the trachea was lifted, a cut was made perpendicular to the length of the tube. A 2mm plastic (what kind of plastic) tube is scraped with a scalpel and inserted into the distal end of the cut trachea about for a centimeter. A piece of 4 gage suture was used to tie off the tube to the trachea. The tube was attached to the 994600 series respirator (TSE Systems) (shown in Figure 2.1) and the breath and CO_2 monitor (shown in Figure 2.2). The animal was then turned over and placed in the stereotaxic frame (shown in Figure 2.3).

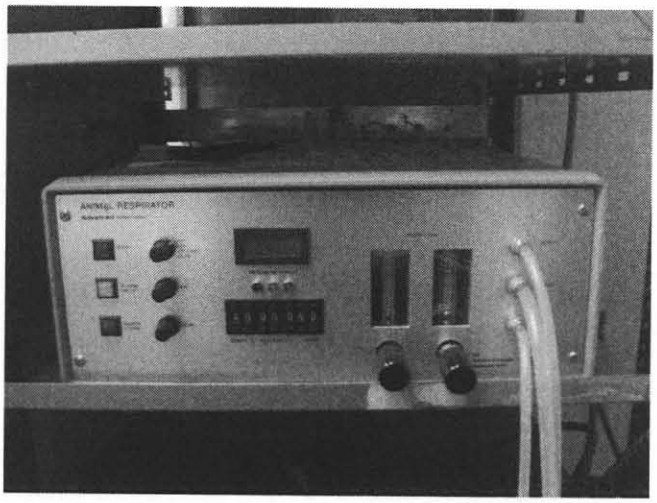

Figure 2.1 The respirator used to control breathing (994600 series Technical & Scientific Equipment (TSE) systems).

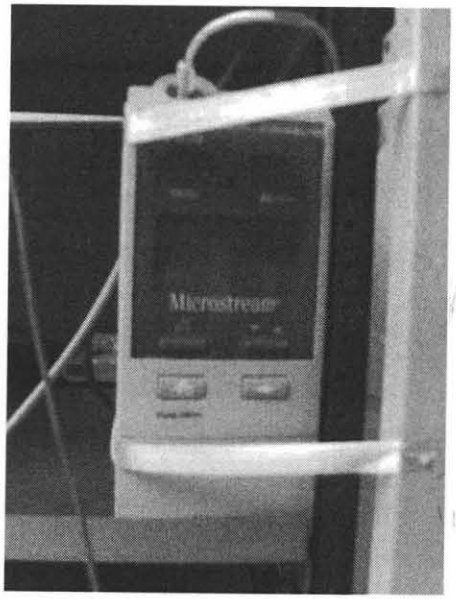

Figure 2.2 End tidal CO_2 and breath rate monitor used to monitor the animals CO_2 (model NFB-70, Microstream).

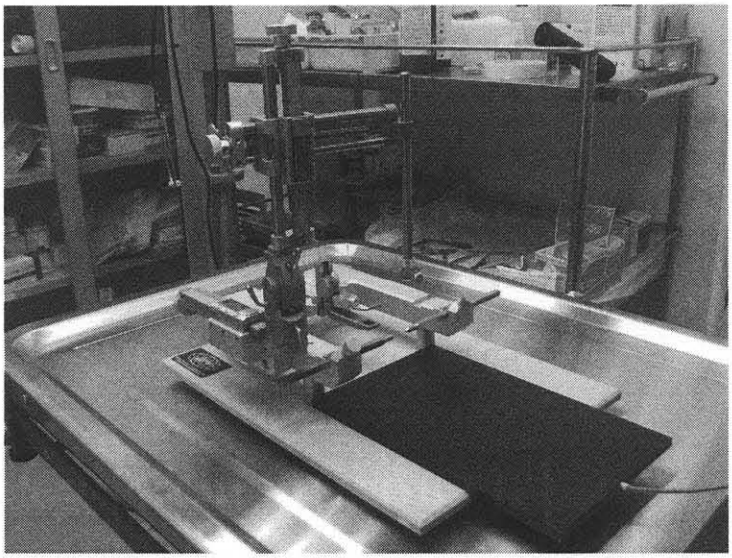

Figure 2.3 The stereotaxic frame used to hold the animal's head under anesthesia during the experiment and the heating pad used to control the animal's temperature (WPI).

The skull above the cerebellum was exposed by cutting down the mid line of the back of the skull, the muscle was then cut away and the skin is reflected back exposing the skull. The skin was held in place by tying suture to the skin and taping it to the stereotaxic frame. The scalpel was used to make a hole in the scull by gently spinning it slowly drilling a hole. A fine tweezers was then used to expand the hole by breaking off small parts of the skull. After the skull was opened enough to allow the corneoscleral punch in, it was used in the place of the tweezers to expand the hole. The hole was expanded to approximately 3X3mm across exposing the cerebellum. After the hole was expanded to the desired radius, a fine 27 gage needle was bent at the tip to a 90 degree angle and used to puncture the dura matter. After the durra matter was punctured the recording array electrode (FlexMEA, Multichannel Systems) was slid under the dura matter over the paramedian lobule.

2.3 Experimental Setup

Figure 2.4 shows the flow diagram of the stimulation and record scheme used in the experiments. LabVIEW was used to control the stimulation of the central and peripheral sites and recording the evoked signals. The stimulator was a voltage to current converter. Two amplification stages were used. The first was a 100 gain amplifier. The second amplifier and low pass filter used had a gain of 10 and a cut off frequency of 5.6 kHz. A National Instruments connector box was used to connect to a National Instruments PCI 6701 data acquisition (DAQ) board. This set up was used for both the stimulation of the periphery and the primary motor cortex.

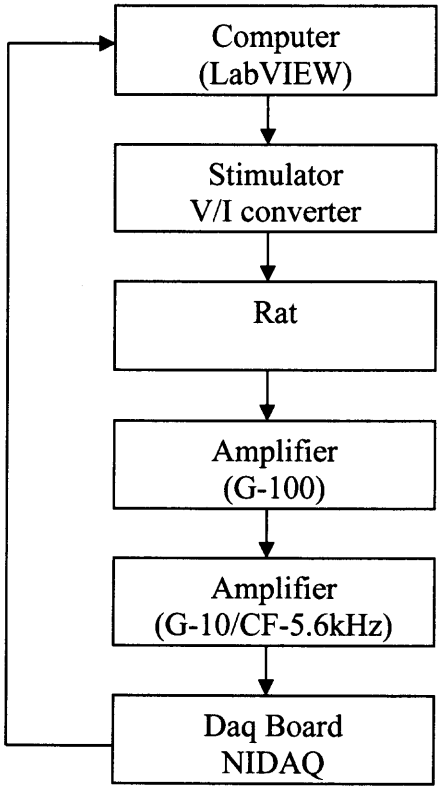

Figure 2.4 The flow diagram of the stimulation and recording scheme used in the experiments.

2.3.1 Signal Acquisition

Signal acquisition parameters were controlled how? The data points were saved to a file using LabVIEW. Twenty eight channels were recorded for the peripheral stimulation and 32 channels were recorded for the central stimulation. Digital to analog conversion was performed with a National Instruments PCI 6701 data acquisition (DAQ) board. The signals were connected to the DAQ board using a National Instruments connector box shown in figure 2.5. The signals were recorded at a sampling frequency of 20 kHz. The input range was set to -2.5V to 2.5V. The signals were acquired for 200ms. To decrease noise, a Faraday cage, shown in figure 2.6 was placed around the animal, the amplification stages, the connector box, and the voltage to current converter. The heating element was turned off and the connection wires were disconnected and the voltage to current converter was disconnected from the AC power supply to further reduce noise.

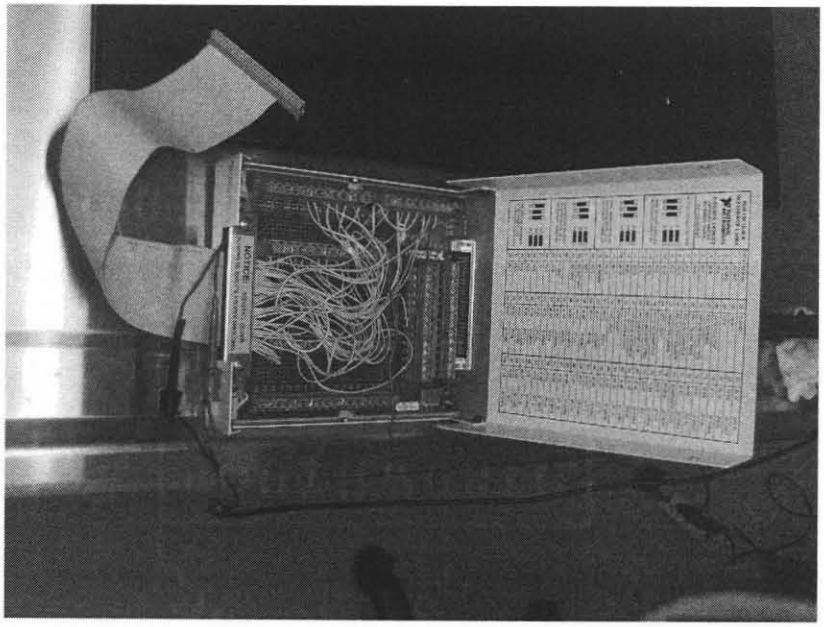

Figure 2.5 National Instruments SCB-100 connector box used to connect the electrode array and amplifiers to the data acquisition board.

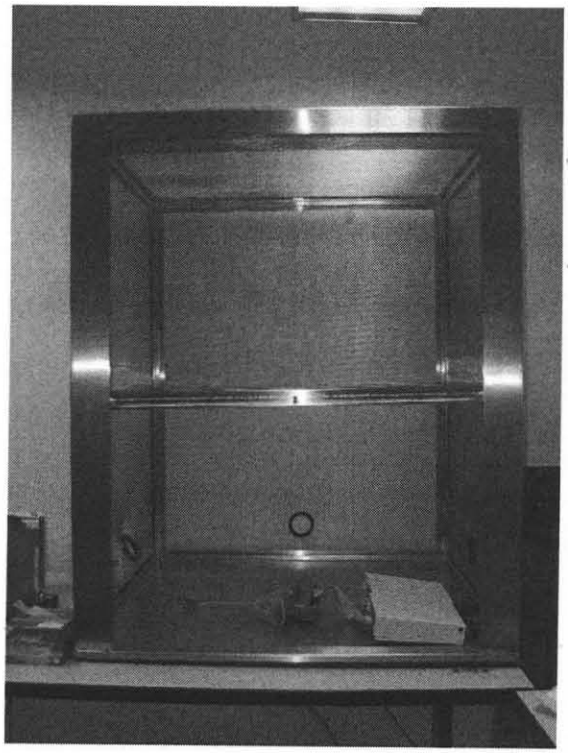

Figure 2.6 Faraday cage used to reduce noise.

2.3.2 Stimulation Procedure

Two stimulation paradigms were used in the experiments. The first paradigm was used for the stimulation of the peripheral afferents. The second paradigm was used in the stimulation of the primary motor cortex. The stimulation paradigms were controlled using LabVIEW software and were generated through the National Instruments DAQ board and the analog stimulus isolator. Both stimulation paradigms used anodic stimulation. The individual stimulation paradigms are described in the following sections.

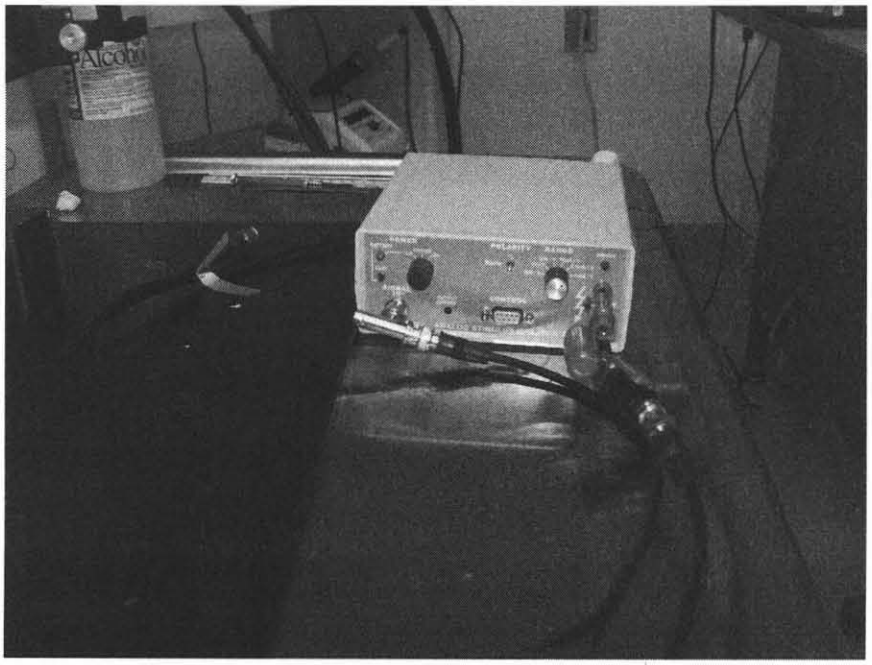

Figure 2.7 The analog stimulus isolator (model 2200, A-M Systems) used in the stimulation for both peripheral and central stimulation.

2.3.2.1 Peripheral Nervous System Stimulation. Peripherally evoked signals were generated by stimulating the afferent fibers, connected to the spinocerebellar pathways, in the muscle of the region that was to be studied. The stimulating electrode was placed intramuscularly in the region of interest by manual insertion. A ground was placed into

the muscular tissue a short distance away. The stimulating and recording electrode were connected to the analog stimulus isolator. The analog stimulus isolator was connected to output of the Daq board Stimulation Parameters were controlled using LabView. Six spikes were used to stimulate the muscle and sensory afferents. Fifty trains of the six spikes were delivered.

2.3.2.2 Central Nervous System Stimulation. Centrally evoked signals were generated by stimulating the primary motor cortex. The six spikes were used to locate the region of interest. During stimulation the area was observed for movement. After the site was located the stimulation was switched to a single spike.

2.3.3 Micro-Array Electrode

The recording electrode array used in the experiments was a FlexMea 300/30 electrode array from Multichannel Systems. The FlexMea has 32 recording contacts arranged in a 6x6 array, the upper corner positions in the array are empty and the lower corner positions in the array are used for reference. Each recording contact is 30μm in diameter and is coated in titanium nitride. The pitch between electrodes is 300μm. There are 2 reference electrodes and 2 grounding pads. The leads going from the recording contacts to the connecting contacts are made of gold and the structural material is made of polyimide 2611 foil. A full size view of the FlexMea is shown in figure 2.6 and a zoomed in view of the contacts is shown in figure 2.7.

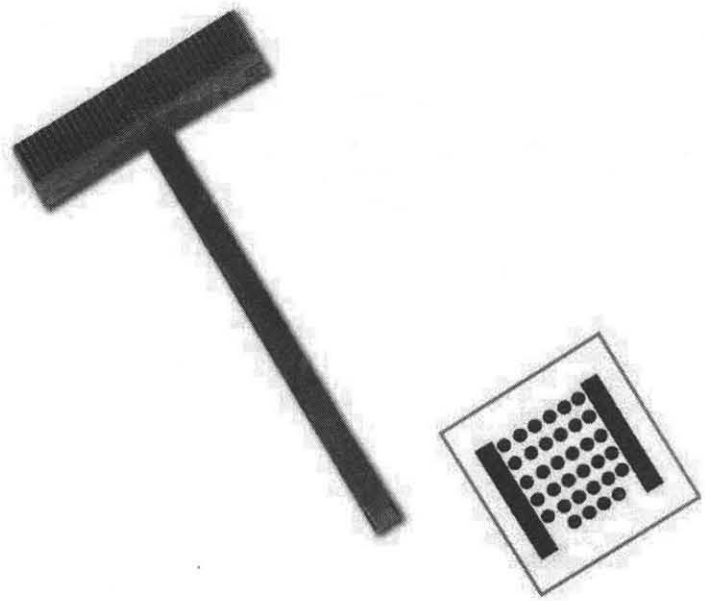

Figure 2.8 The FlexMea electrode (www.multichannelsystems.com).

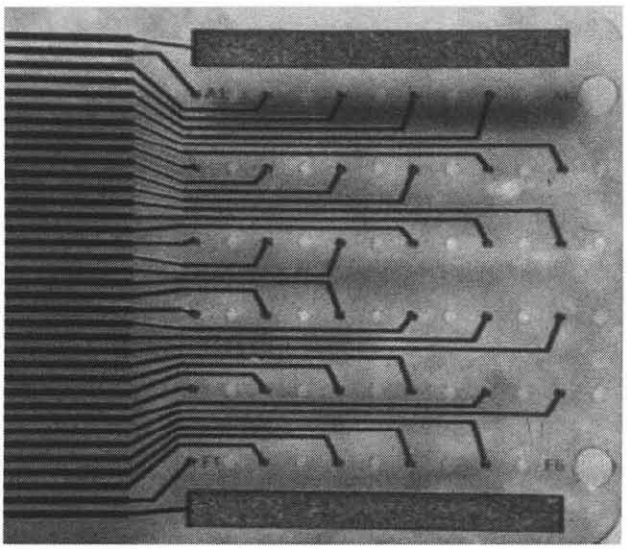

Figure 2.9 The FlexMea array contacts with 32 recording electrodes, 2 reference electrodes, and 2 grounding pads (www.multichannelsystems.com).

2.3.4 Amplifiers

2.3.4.1 Head Stage Amplifier. The first stage of amplification was performed through a T3G100 head stage amplifier from Triangular Biosystems Inc (address). The T3G100 amplifier is a VSLI amplifier with 32 channels and a gain of 100. The amplifier is able to operate on a 3V and 5V power supply. It is 16 mm in width, 23 mm in length and, 5 mm in height. Its weight is less than 0.8 grams. The input and output stages are connected through Omnetics connectors.

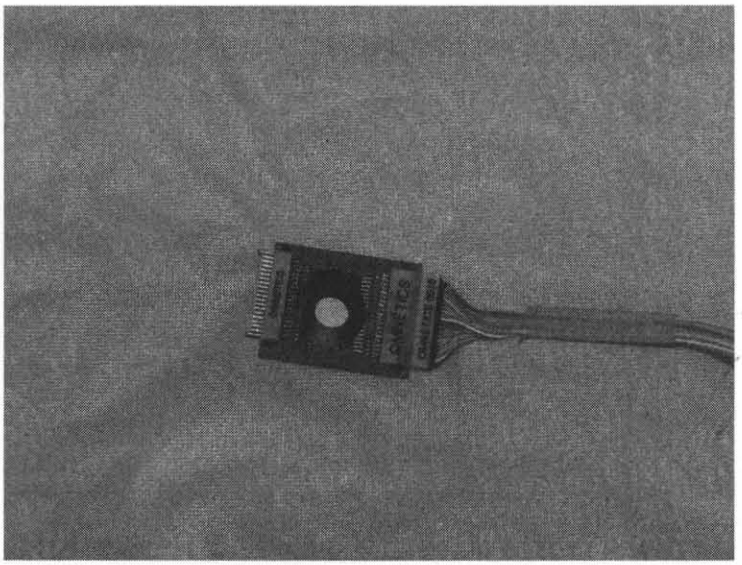

Figure 2.10 The T3G100 amplifier.

2.3.4.2 Amplifier and Anti-aliasing Filter. The second stage of amplification used an LM324 operational amplifier. The gain of the amplification stage was 10. The cut off frequency of the low pass filter was 5.6 kHz.

2.4 Signal Processing

The data were processed offline using MatLab. The peripherally evoked signals were acquired 50 times and the centrally evoked signals were acquired 100 times for averaging. The signals were recorded for a duration of 200ms per stimulation. The signals were spike-trigger averaged using the time of stimulation as the triggering parameter. The amplitude and index of the peaks of the N1 wave and the positive inflexion between the N3 and N4 peaks were recorded. The values of the difference of the two peaks were mapped to the electrode location on the array. There was a high degree of variability of the time of onset of the signal observed in the individual samples, so in order to obtain samples for statistical analysis of the difference between two sites of stimulation, a model signal was taken and shifted through each sample, point by point for each sample stimulation (???). The model signal was correlated with the original signal. The maximum correlation was found and the index of the maximum was recorded.

2.4.1 Spike-Triggered Averaging

The signals were recorded at regular intervals. Therefore the time of stimulation that corresponded to the start of recording was used as the triggering parameter. All of the recording durations were contained in a single file so the length of the recordings was calculated to separate each acquisition. This was done by using the sampling frequency of 20kHz and multiplying it by the recording duration of 0.2s. The multiple acquisitions were added together using a *for* loop.

2.4.2 Measurement

Measurements of the N1 peak and the positive inflection were taken manually. The value at the peaks and the index of the value were recorded. Figure 2.11 shows a sample signal and the arrows show the peaks were the value was recorded.

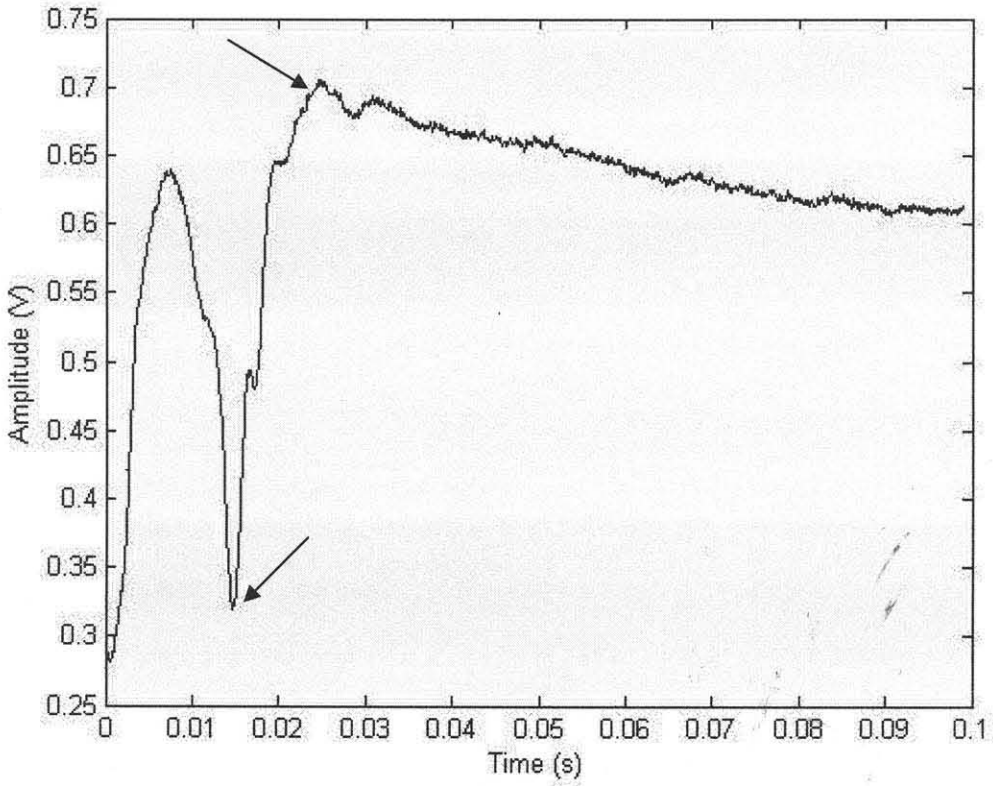

Figure 2.11 Sample picture of the field potential evoked by stimulating the forearm region of the M1 cortex. The arrows show the two peaks measured.

2.4.3 Mapping

The difference between the two amplitudes was taken and placed in the array. The amplitudes were mapped out into the positions in the array of the electrodes. The amplitudes were then graphically represented by plotting them using the *surface* function in MatLab.

2.4.4 Analysis of Variance (ANOVA)

The signals were normalized in order to compare the regions of activity for each stimulation site. The amplitudes were normalized by dividing each sample for each electrode by the square root of the summation of the square of the 100 amplitudes for each sample.

The ANOVA analysis was performed using the manova1 function. The variables g and h are the groups 1 and 2 which correspond to the first stimulation site X and the second stimulation site Y being compared. The variable p was the p-value given by the ANOVA. The variable d was a Boolean variable with a value of 1 representing the hypothesis that the means were the same can be rejected and a value of 0 representing that the hypothesis cannot be rejected. The ANOVA analysis was done independently for each electrode site giving a d and p value for each electrode.

CHAPTER 3

RESULTS

3.1 Cerebellar Field Potentials Evoked by Peripheral Stimulation

The peripherally evoked field potentials were evoked using intramuscular stimulation. The stimulating electrode was placed in the muscle of the region of interest. For each stimulation site, 49 recordings were taken.

The peripherally evoked signals showed both mossy fiber and climbing fiber field potentials which are shown in Figure 3.1. The mossy fiber signal arrived approximately 1.4ms after stimulation. The climbing fiber signal followed, approximately 10ms after stimulation.

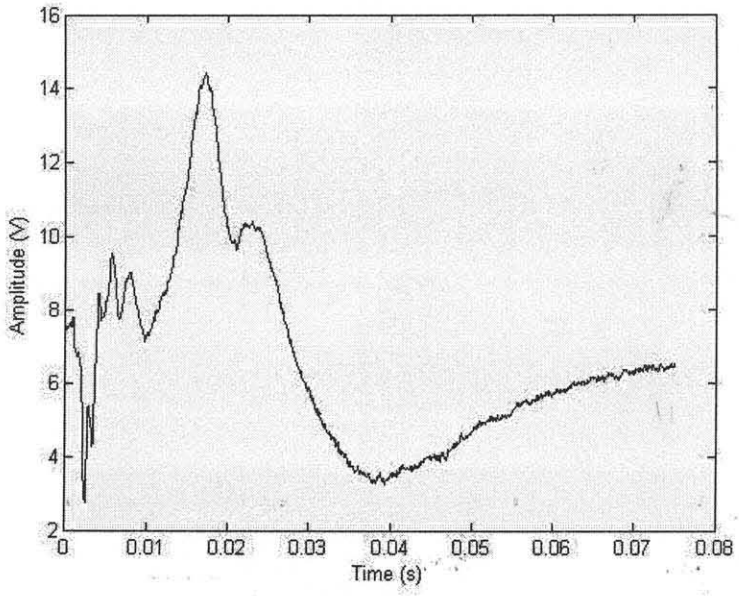

Figure 3.1 Shows the mossy fiber and climbing fiber potentials from channel 28 evoked through peripheral stimulation of the ipsilateral vibrissa.

The peripherally evoked signals showed the P1, N1, N2, N3, N4, and P4 components of the mossy fiber potential. The mossy fiber field potential arrived about 1.4ms after the stimulation, showing a short latency after. The arrival time of the N1 peak averaged 2.3

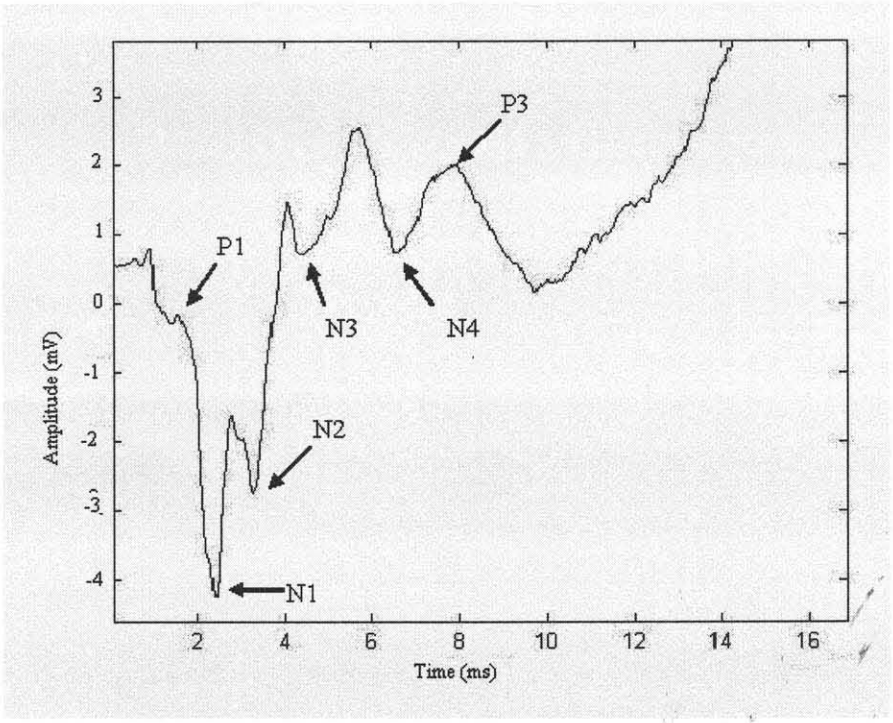

Figure 3.2 Shows the mossy fiber potential from channel 28 evoked through peripheral stimulation of the ipsilateral vibrissa. The mossy fiber potential showed a short latency of arrival at 1.4ms after the stimulation. The arrows show the P1, N1, N2, N3, N4, and P3 waves.

The climbing fiber field potential arrived at about 10 ms after stimulation which was in line with the results found by peripheral stimulation found by Armstrong et al. The climbing fiber potential also showed larger amplitude than that of the mossy fiber field potential. The climbing fiber field potential showed a two component potential field with similar shape found by Armstrong et al.

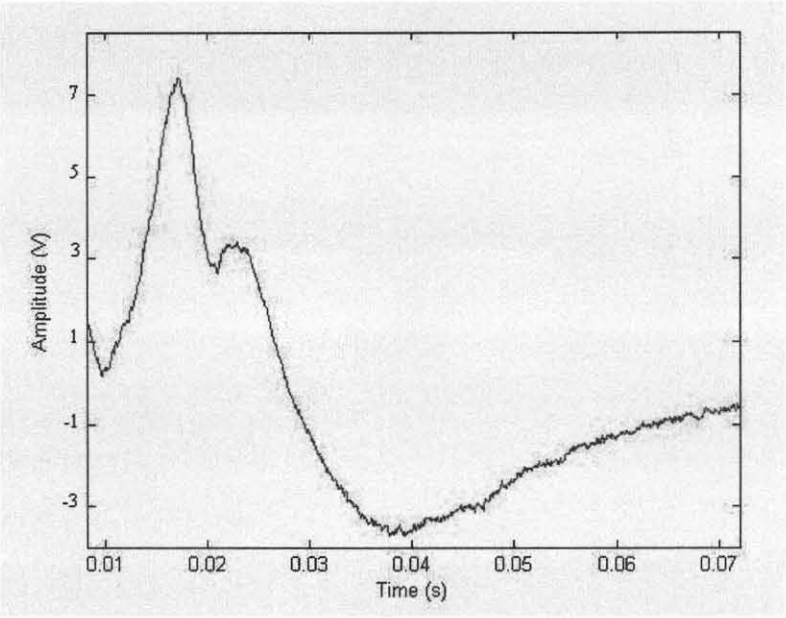

Figure 3.3 Shows the climbing fiber potential from channel 28 evoked through peripheral stimulation of the ipsilateral vibrissa. The climbing fiber field potential arrives at 10ms after stimulation and had amplitude larger than that of the mossy fiber potential. This graph shows that the climbing signal was not a simple field potential but rather had two components, the first is a large positive wave followed by a smaller biphasic wave.

3.2 Cerebellar Field Potentials Evoked by Central Stimulation

The centrally evoked potentials were produced by stimulating the primary motor cortex. The recordings were taken from the paramedian lobule of the cerebellar cortex. One hundred recordings were taken for each stimulation site. The signals were recorded for 200ms. Action producing stimulation was achieved for the forearm, jaw, elbow, and whiskers in one rat. The signals that showed the mossy fiber field potential in at least one channel were chosen for analysis.

The centrally evoked potentials contained only the mossy fiber component. The mossy fiber signal had same components and shape as the peripherally evoked potentials with the same P1, N1, N2, N3, N4 waves that were present in the peripherally evoked potentials. Even though the shape and components of the centrally evoked potentials

were similar to the peripherally evoked potentials, the duration of the centrally evoked potentials were longer and had broader wave forms. An example of a centrally evoked potential is shown in Figure 3. 4.

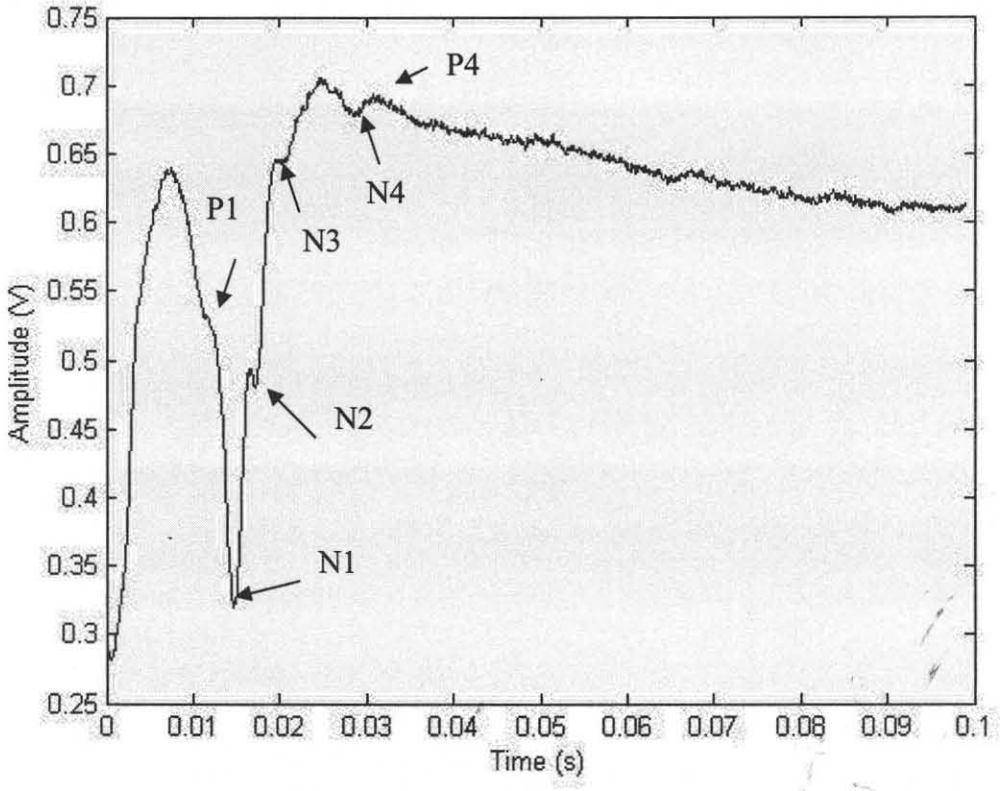

Figure 3.4 Mossy fiber field potential from the cerebellum evoked by stimulation of the forearm region of the primary motor cortex. Arrows show the P1, N1, N2, N3, N4, and P4 components of the mossy fiber signal.

The amplitudes of the signal were quantified by using the values at the N1 wave trough and the peak of the positive inflection between the N3 and N4 waves. These points are shown by the arrows in Figure 3.5. When the peaks were not discernable the first negative and positive peaks were used. The difference of the two peaks was taken subtracting the negative peak from the positive peak. The amplitudes of the signals for each electrode were mapped to their place in the array.

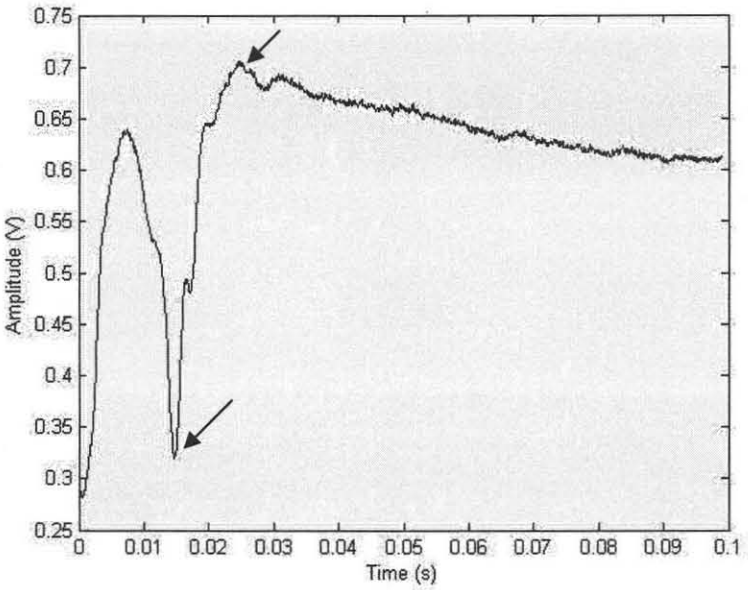

Figure 3.5 Arrows show the peaks were the values were taken for the amplitude measurements. For signals were the peaks were not discernable the first negative and the following positive inflection were used for the amplitudes.

3.2.1 Forearm Area Stimulation

The forearm stimulation was generated by stimulating primary motor cortex at the coordinates 1.2 mm from the bregma in the anterior-posterior (AP) direction and 3.0mm from the bregma in the medial-lateral (ML) direction. The region was stimulated at amplitude of 200μA. The forearm area evoked potentials showed all the components of the mossy fiber signal after spike-triggered averaging.

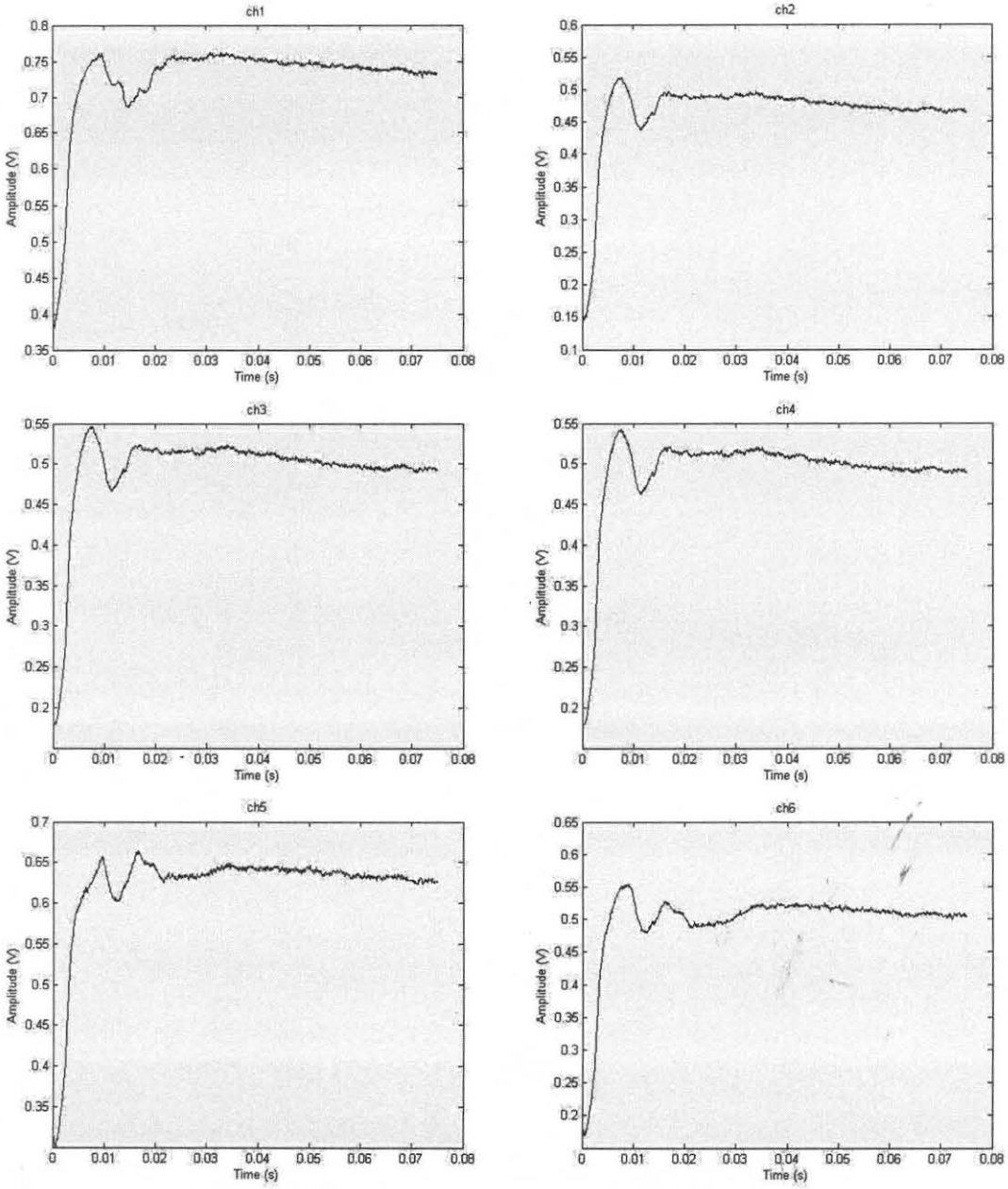

Figure 3.6 The spike-trigger averaged field potentials for channels 1 though 6 evoked by stimulating the forearm region of the primary motor cortex.

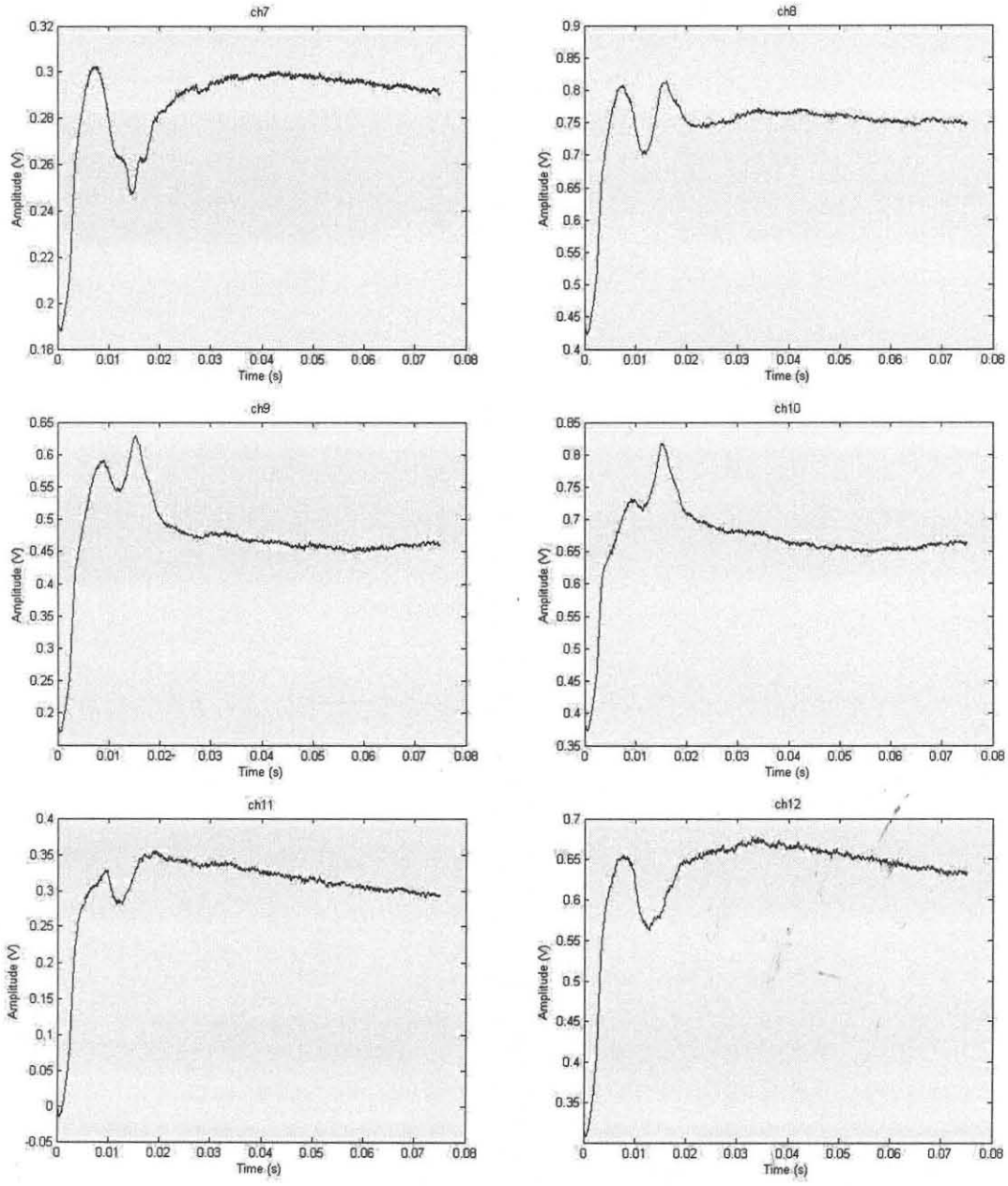

Figure 3.7 The spike triggered averaged field potentials for channels 7 though 12 evoked by stimulating the forearm region of the primary motor cortex.

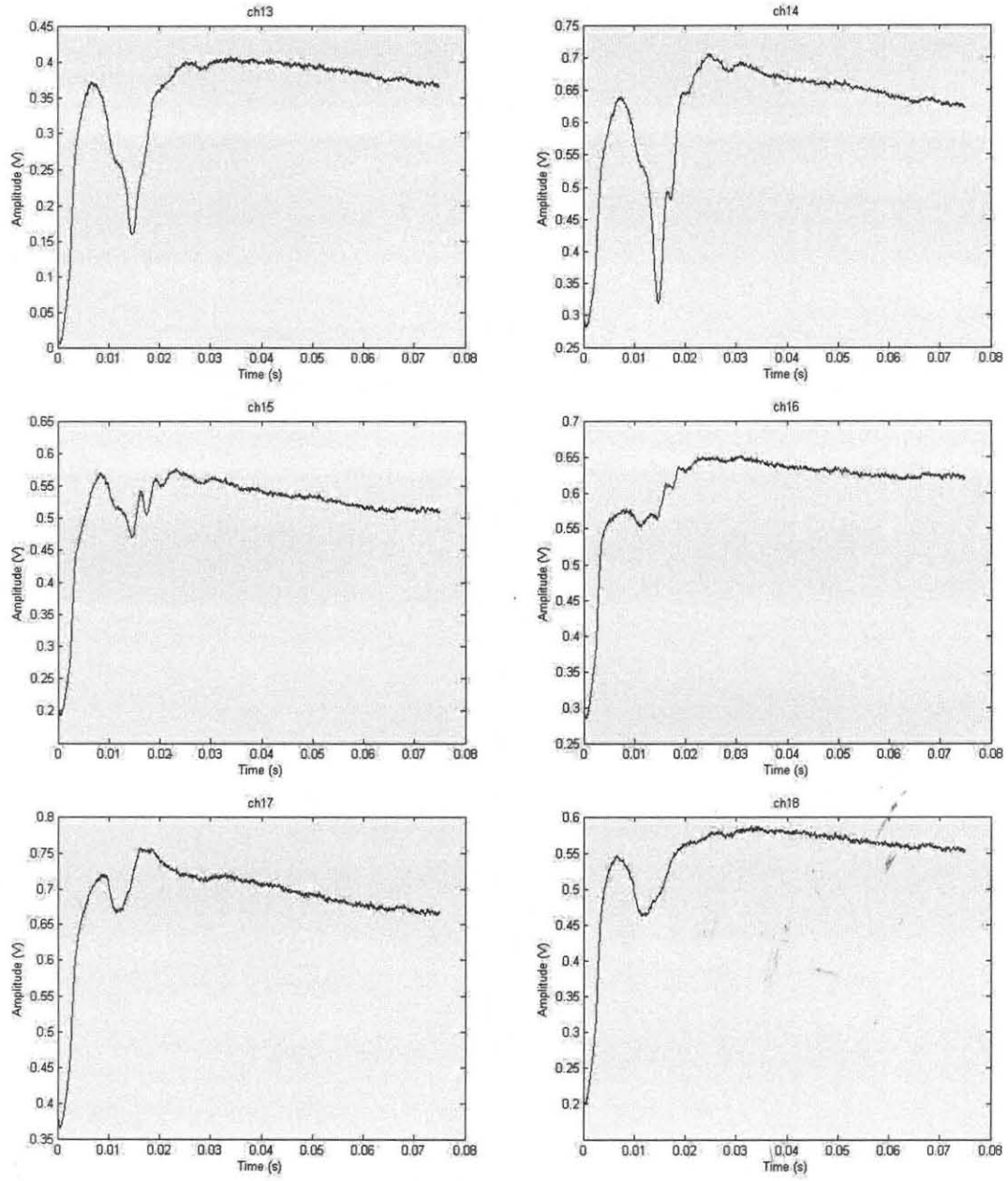

Figure 3.8 The spike triggered averaged field potentials for channels 13 though 18 evoked by stimulating the forearm region of the primary motor cortex.

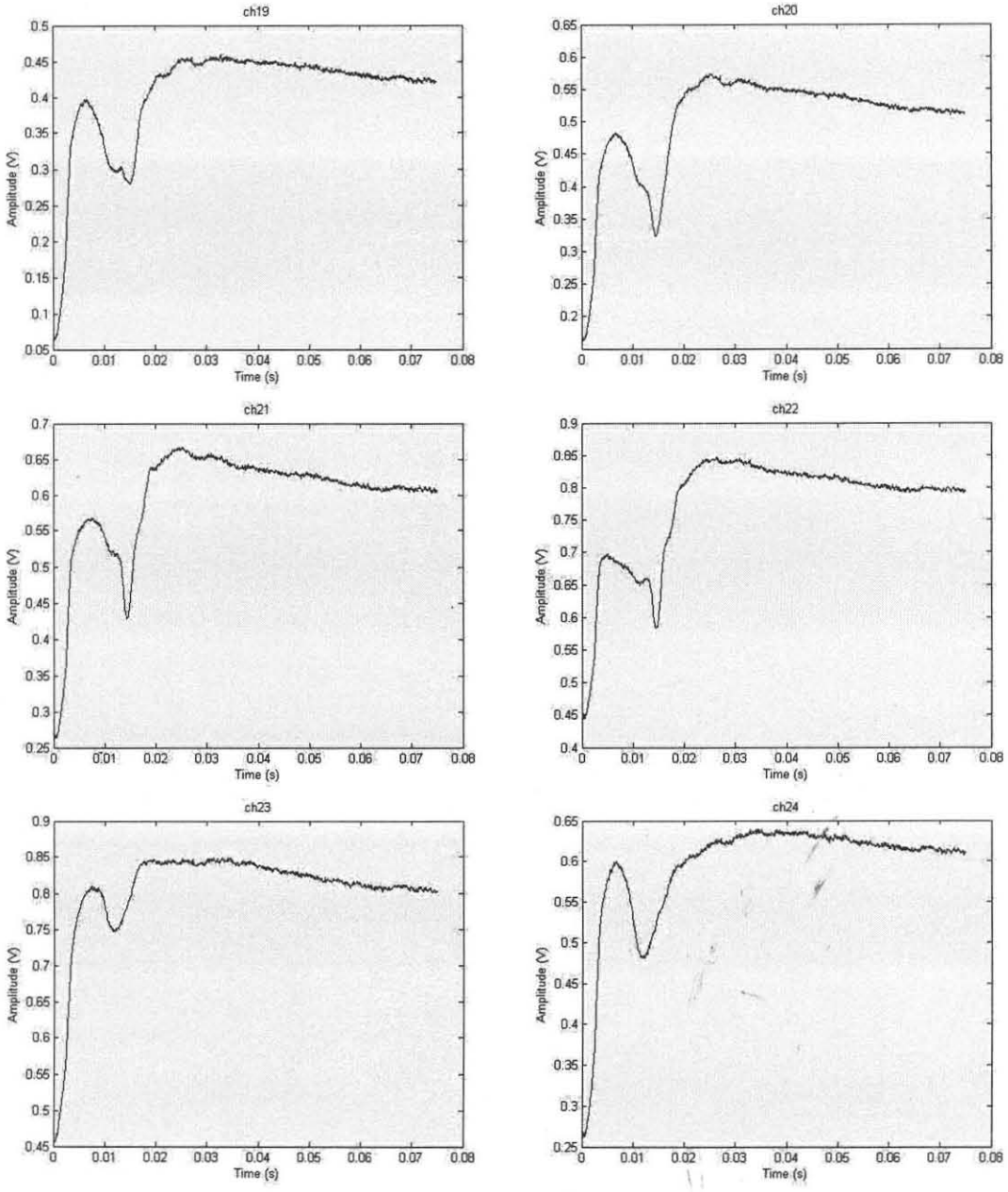

Figure 3.9 The spike triggered averaged field potentials for channels 19 though 24 evoked by stimulating the forearm region of the primary motor cortex.

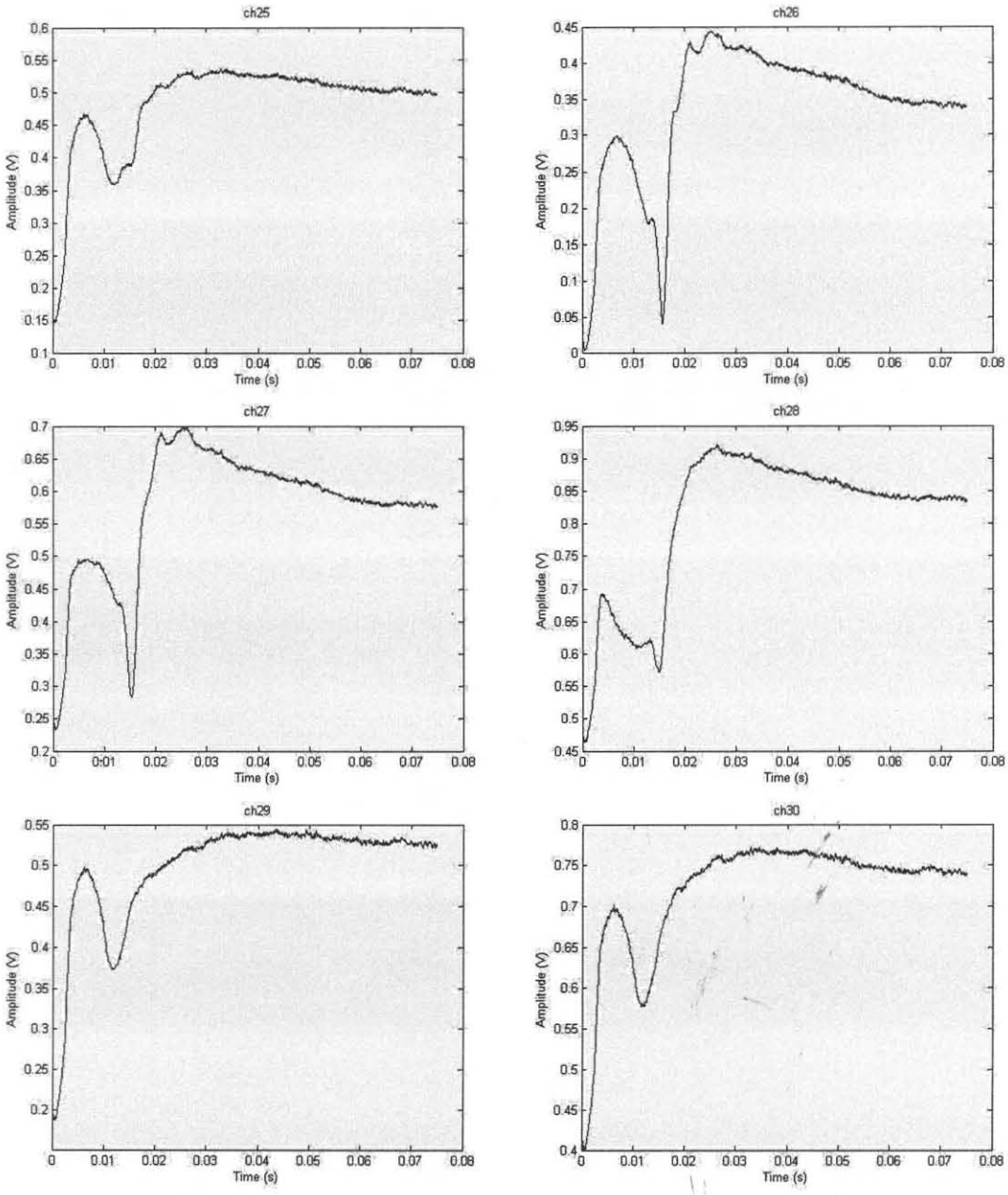

Figure 3.10 The spike triggered averaged field potentials for channels 25 though 30 evoked by stimulating the forearm region of the primary motor cortex.

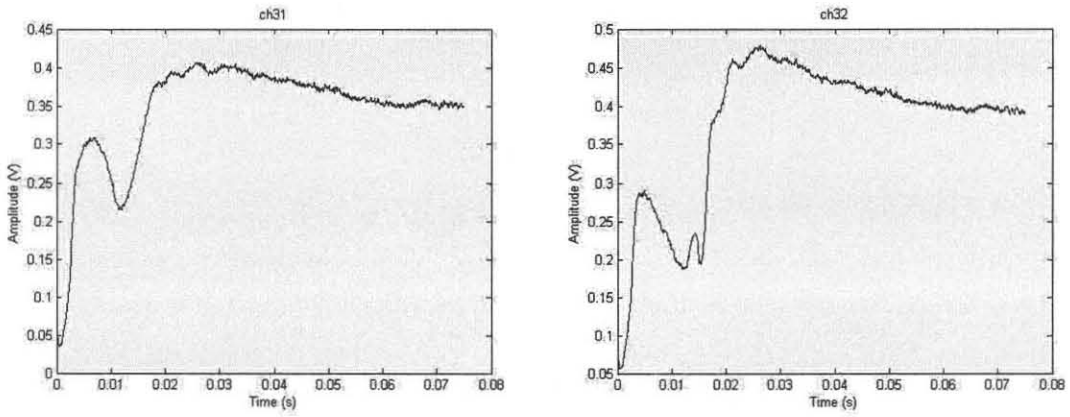

Figure 3.11 The spike triggered averaged field potentials for channels 31 and 32 evoked by stimulating the forearm region of the primary motor cortex.

The map of the forearm evoked potentials showed a region of activity in the lateral-rostral portion of the electrode array. The amplitudes of the averaged signals ranged from 0.5μV to 4μV. The map of the amplitudes arranged to the electrode position is shown in Figure 3.12.

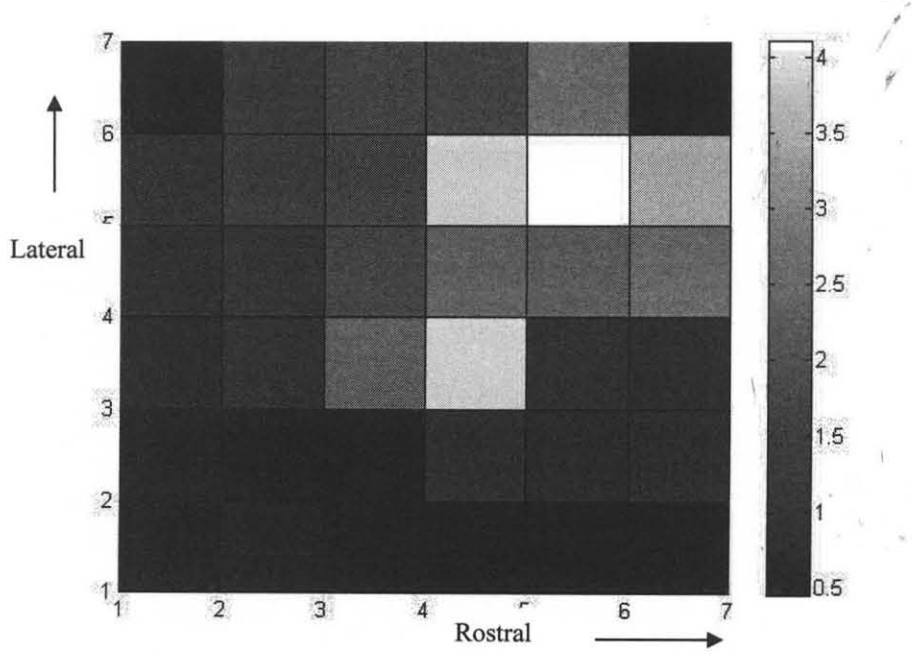

Figure 3.12 The amplitude maps of the forearm region evoked potentials, acquired from the spike triggered averaged signals, showing a region of activity in the rostro-lateral portion. The range of the amplitudes is from 0.5mV to 4mV.

Ten sample recordings taken from the 14th electrode position in the array are shown in Figure 3.13. They demonstrate that there was a large variation in the time of onset between each stimulation cycle. This variation was seen throughout the stimulation cycles. The fourteenth electrode field potentials were chosen as a representative signal because they showed the best signal in the spike triggered averaging although the variation was detected in all electrode positions. The histogram in Figure 3.14 shows the distribution of the time of the N1 wave peak amplitude. The mean of the time of the N1 wave peak amplitude for the samples was 15.7ms with a standard deviation of 1.7ms.

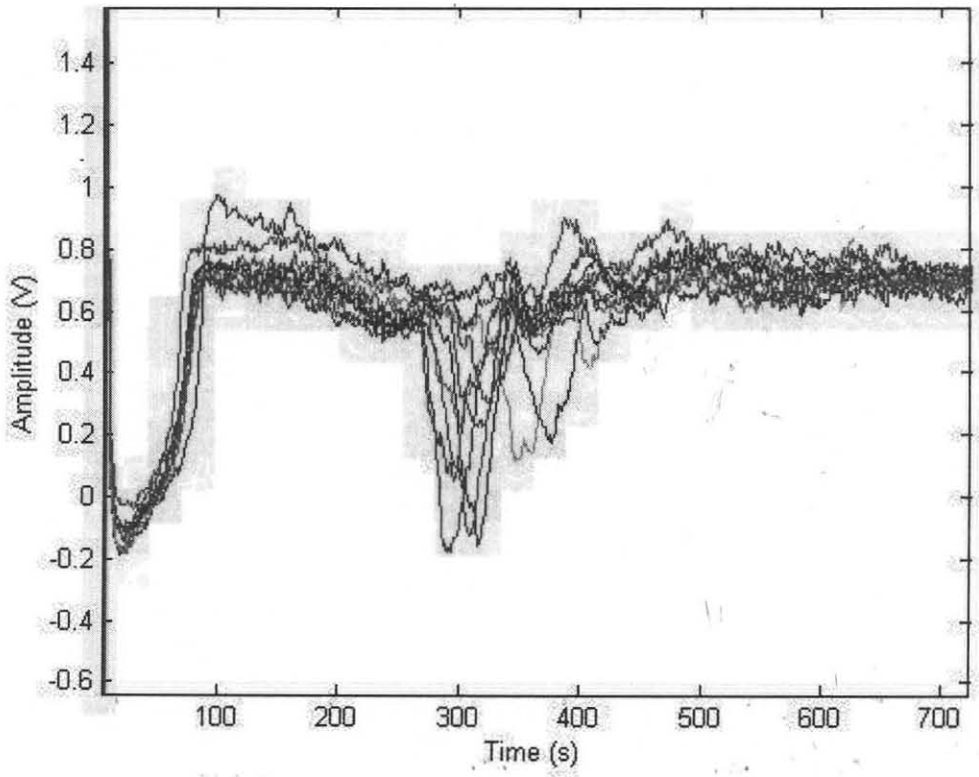

Figure 3.13 The evoked field potentials of first 10 samples recorded from the 14th electrode position in the array for the stimulation of the forearm area of the primary motor cortex. The plots show that the time of onset was not steady from recording to recording.

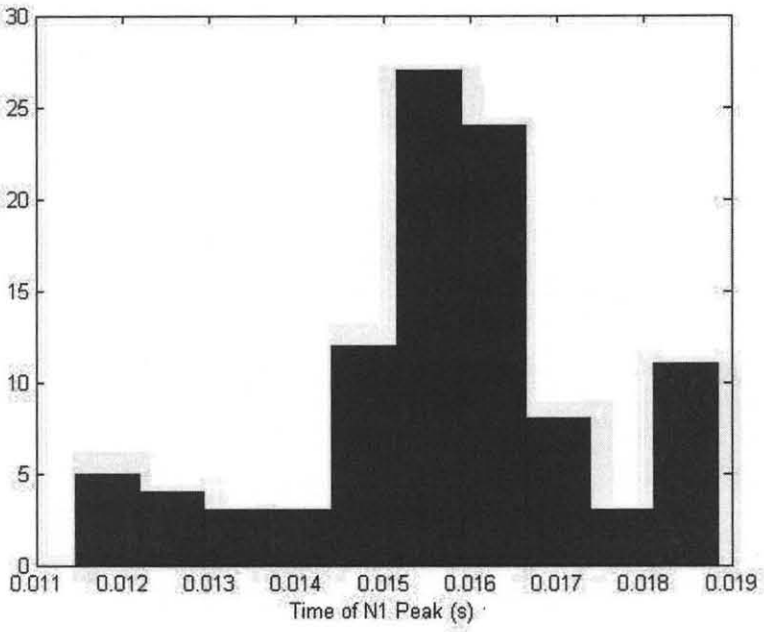

Figure 3.14 Histogram of the time of the N1 wave peak amplitude of the fourteenth electrode position from the stimulation of the forearm area of the primary motor cortex for all 100 samples. The heights of the bars are the number of samples that are in each bin. The mean of the time of the N1 wave peak amplitude was 15.7ms and the standard deviation was 1.7ms.

3.2.1 Jaw Area Stimulation

Jaw stimulation was generated by amplitude of 100μA shock to the primary motor cortex at the coordinates 1.5mm from the bregma in the anterior-posterior (AP) direction and 3.2mm from the bregma in the medial-lateral (ML) direction. The jaw area evoked potentials were similar to those evoked by stimulation of the forearm area, showing all of the components of the mossy fiber field potential, however the jaw area evoked potentials were much stronger with over twice the amplitude and showing a broader area of activation on the electrode surface.

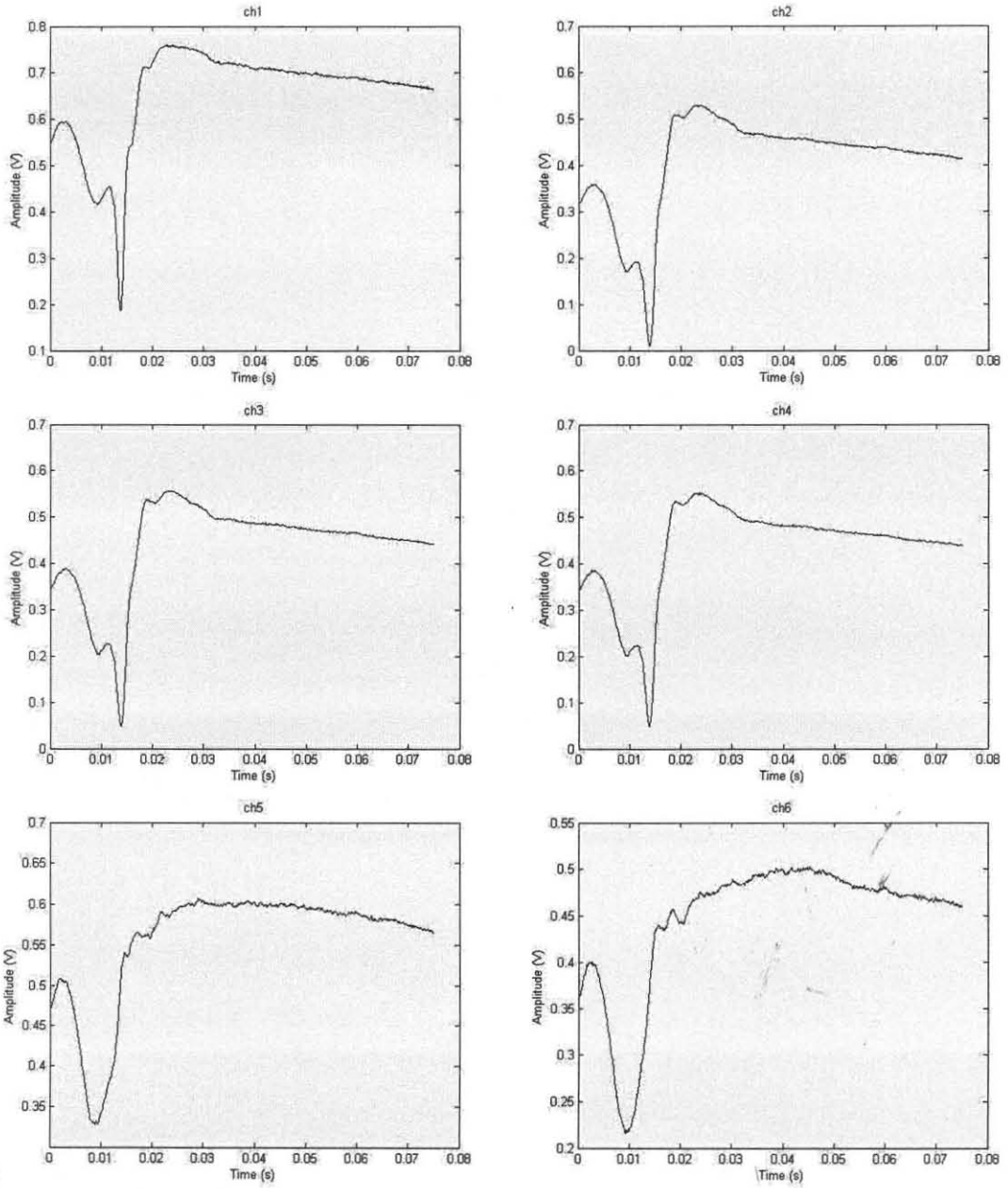

Figure 3.15 The spike triggered averaged field potentials for channels 1 though 6 evoked by stimulating the jaw region of the primary motor cortex.

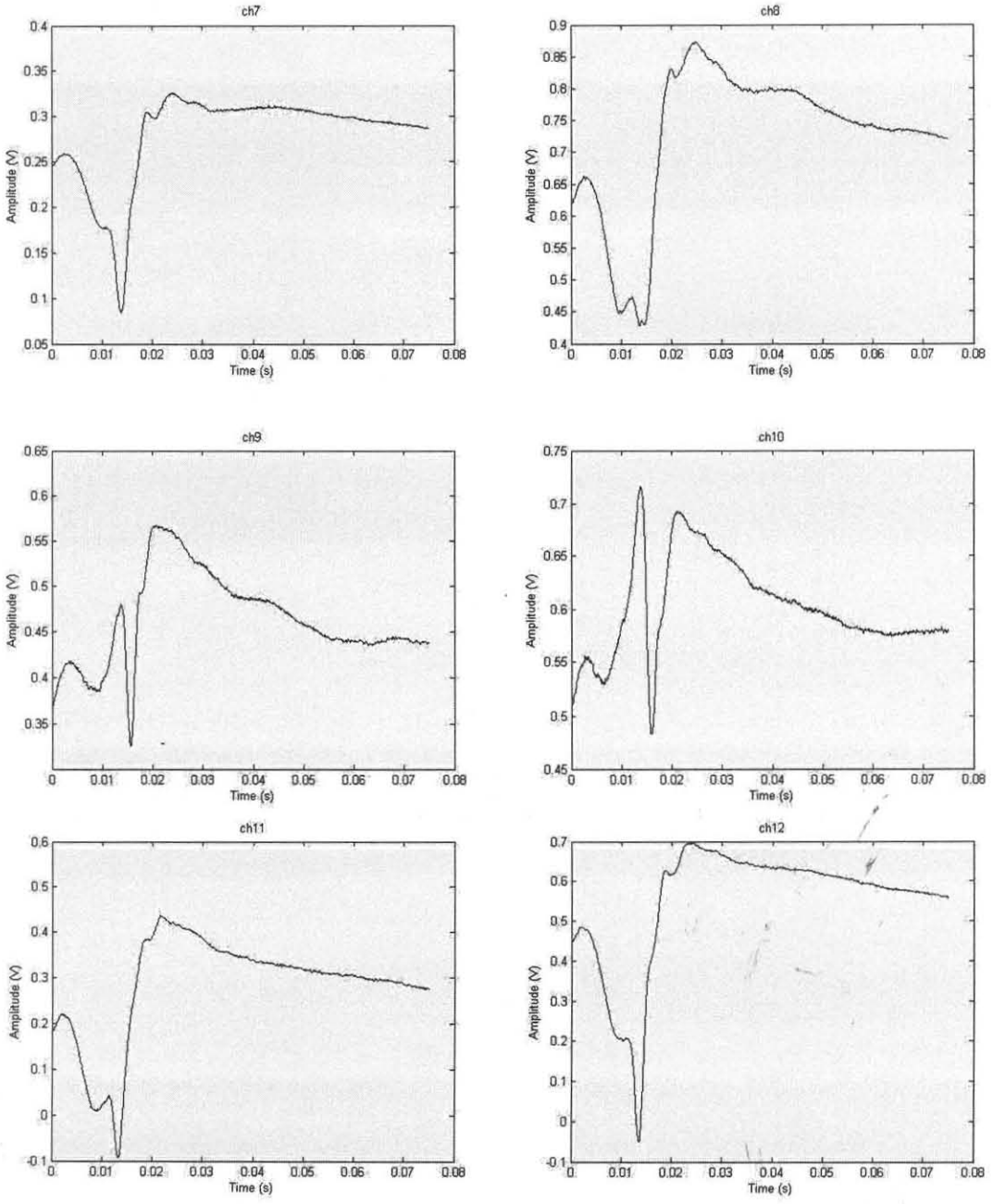

Figure 3.16 The spike triggered averaged field potentials for channels 7 though 12 evoked by stimulating the jaw region of the primary motor cortex.

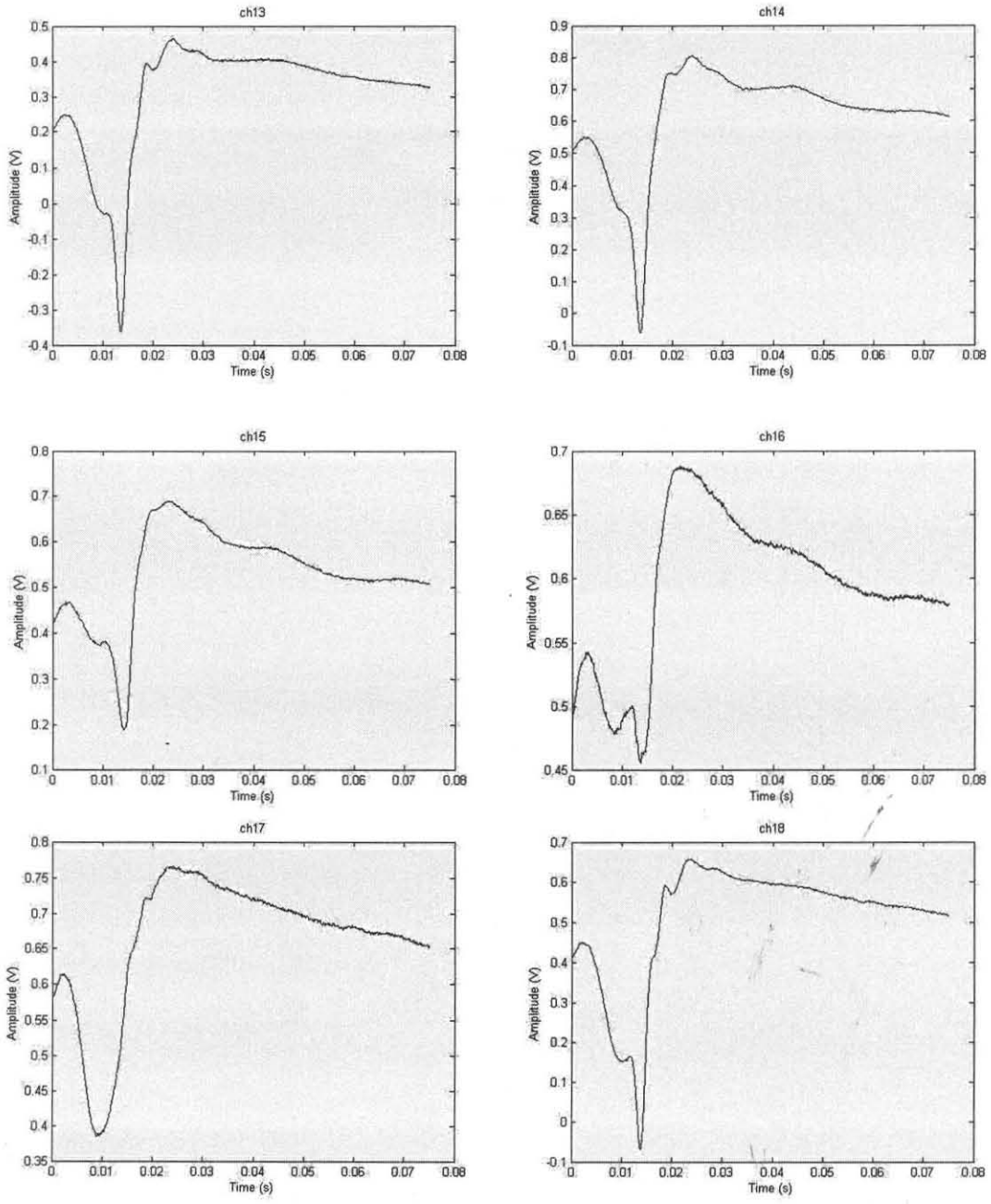

Figure 3.17 The spike triggered averaged field potentials for channels 13 though 18 evoked by stimulating the jaw region of the primary motor cortex.

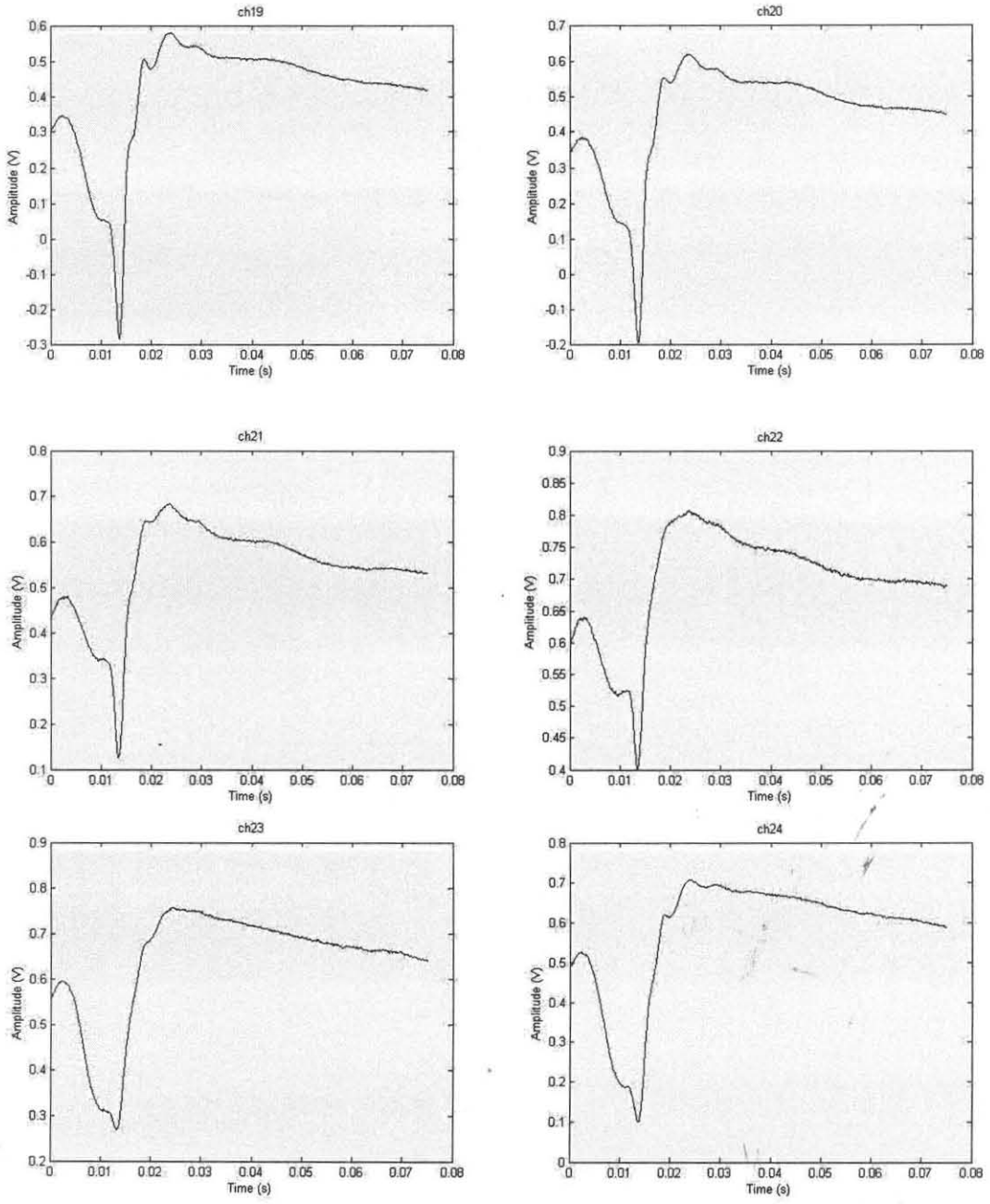

Figure 3.18 The spike triggered averaged field potentials for channels 19 though 24 evoked by stimulating the jaw region of the primary motor cortex.

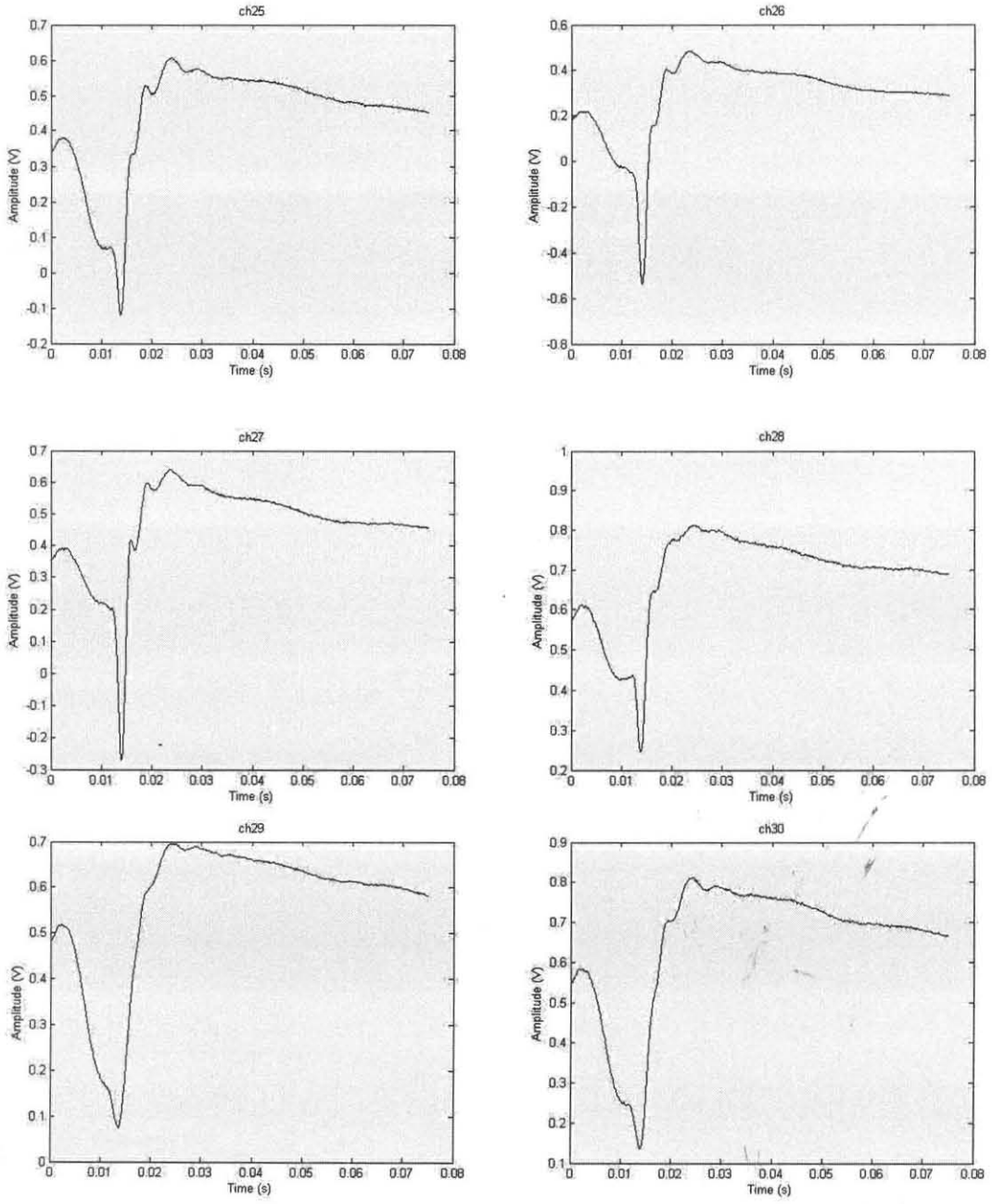

Figure 3.19 The spike triggered averaged field potentials for channels 25 though 30 evoked by stimulating the jaw region of the primary motor cortex.

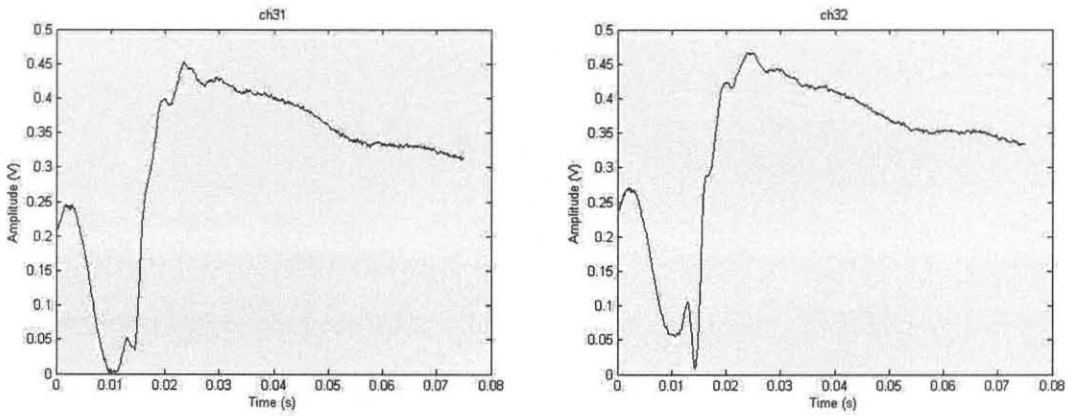

Figure 3.20 The spike triggered averaged field potentials for channels 31 and 32 evoked by stimulating the jaw region of the primary motor cortex.

The sensor map of the jaw evoked potentials showed a region of activity in the middle portion of the recorded area. The amplitudes of the averaged signals ranged from 2mV to 10mV. The map of the amplitudes arranged to the electrode position is shown in Figure 3.21.

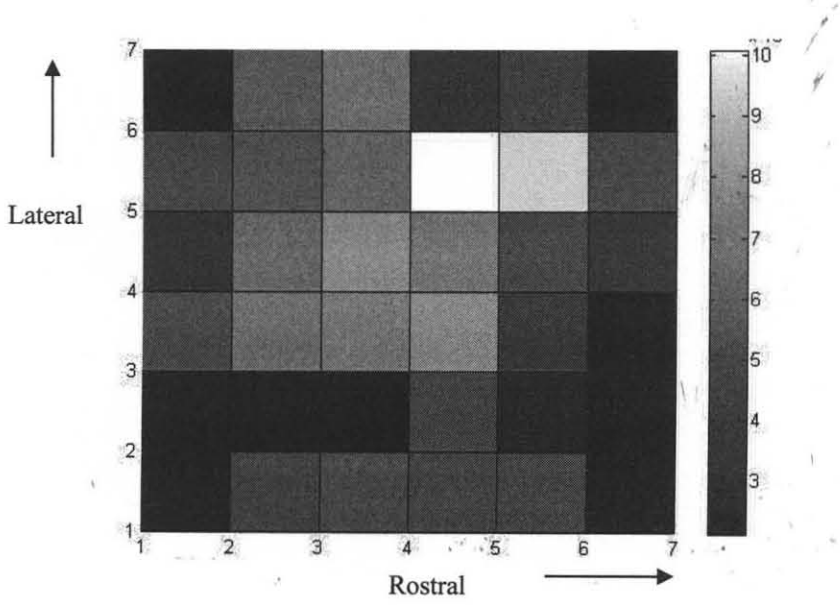

Figure 3.21 The amplitude maps of the jaw region evoked potentials, acquired from the spike triggered averaged signals, showing a region of activity in the middle of the recording area. The range of the amplitudes is from 2mV to 10mV.

A subset of the first ten samples taken from the 26th electrode position in the array are shown in Figure 3.22. The data show that there was a large variation in the time of onset between each stimulation cycle. This variation was seen through out the stimulation cycles. The 26th electrode field potentials were chosen as a representative signal because they showed the best signal in the spike triggered averaging, although the variation was seen in all electrode positions. The histogram in Figure 3.23 shows the distribution of the time of the N1 wave peak amplitude. The mean of the time of the N1 wave peak amplitude for the four was 15.01ms with a standard deviation of 0.72ms.

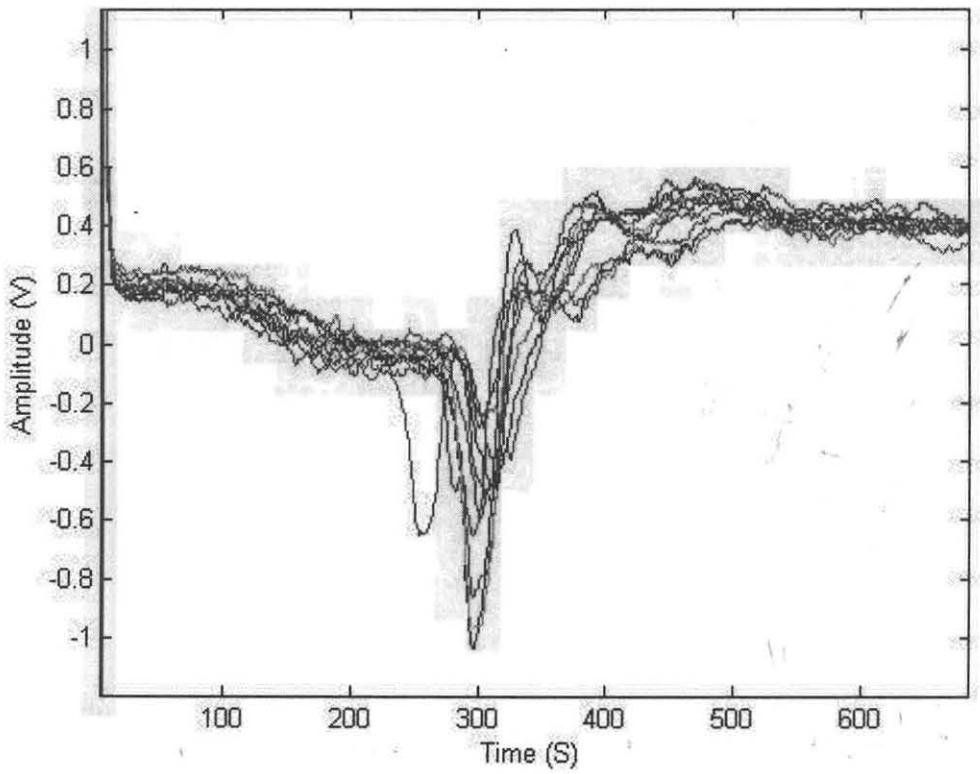

Figure 3.22 The evoked field potentials of first 10 samples recorded from the 14th electrode position in the array for the stimulation of the forearm area of the primary motor cortex. They show that the time of onset was not steady from recording to recording.

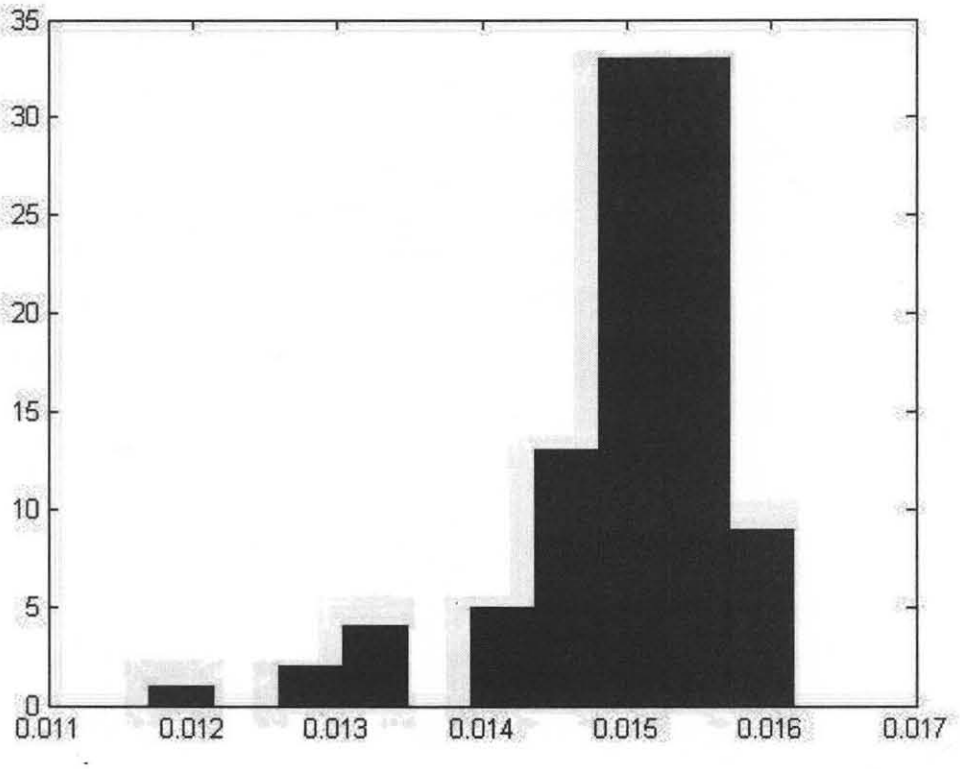

Figure 3.23 Histogram of the time of the N1 wave peak amplitude of the twenty sixth electrode position from the stimulation of the jaw area of the primary motor cortex for all 100 samples. The heights of the bars are the number of samples that are in each bin. The mean of the time of the N1 wave peak amplitude was 15.01ms and the standard deviation was 0.72ms.

3.2.1 Elbow Area Stimulation

Elbow stimulation evoked potentials were generated by stimulating the primary motor cortex at the coordinates 1.5mm from the bregma in the anterior-posterior (AP) direction and 2.0mm from the bregma in the medial-lateral (ML) direction. The region was stimulated at an amplitude of 200μA. The elbow area evoked potentials were similar to those evoked by stimulation of the forearm and jaw area, showing all of the components of the mossy fiber field potential, however the forearm and elbow area evoked potentials were much weaker with over an order of magnitude decrease in amplitude from the potential evoked by the forearm and jaw area.

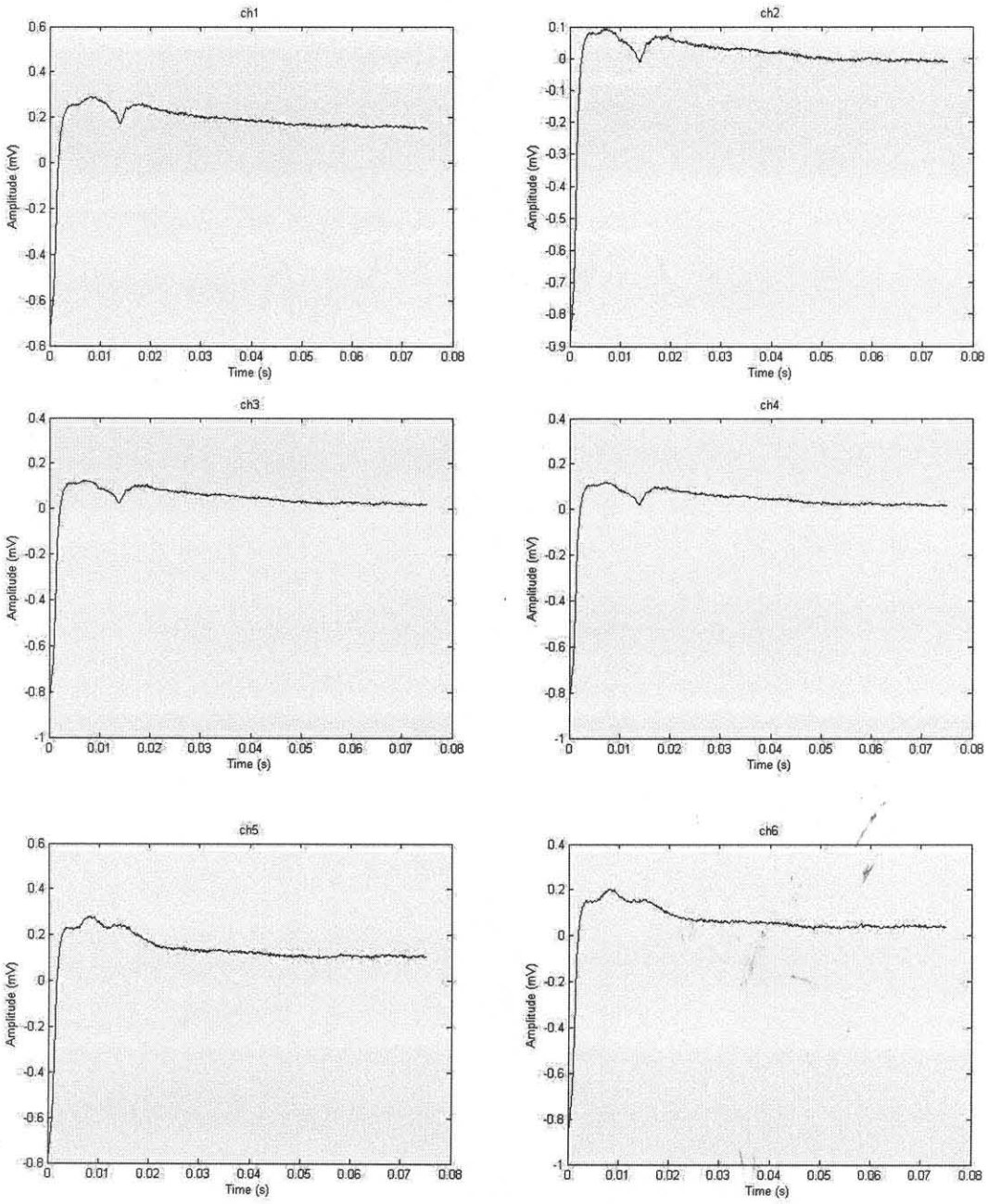

Figure 3.24 The spike triggered averaged field potentials for channels 1 though 6 evoked by stimulating the elbow region of the primary motor cortex.

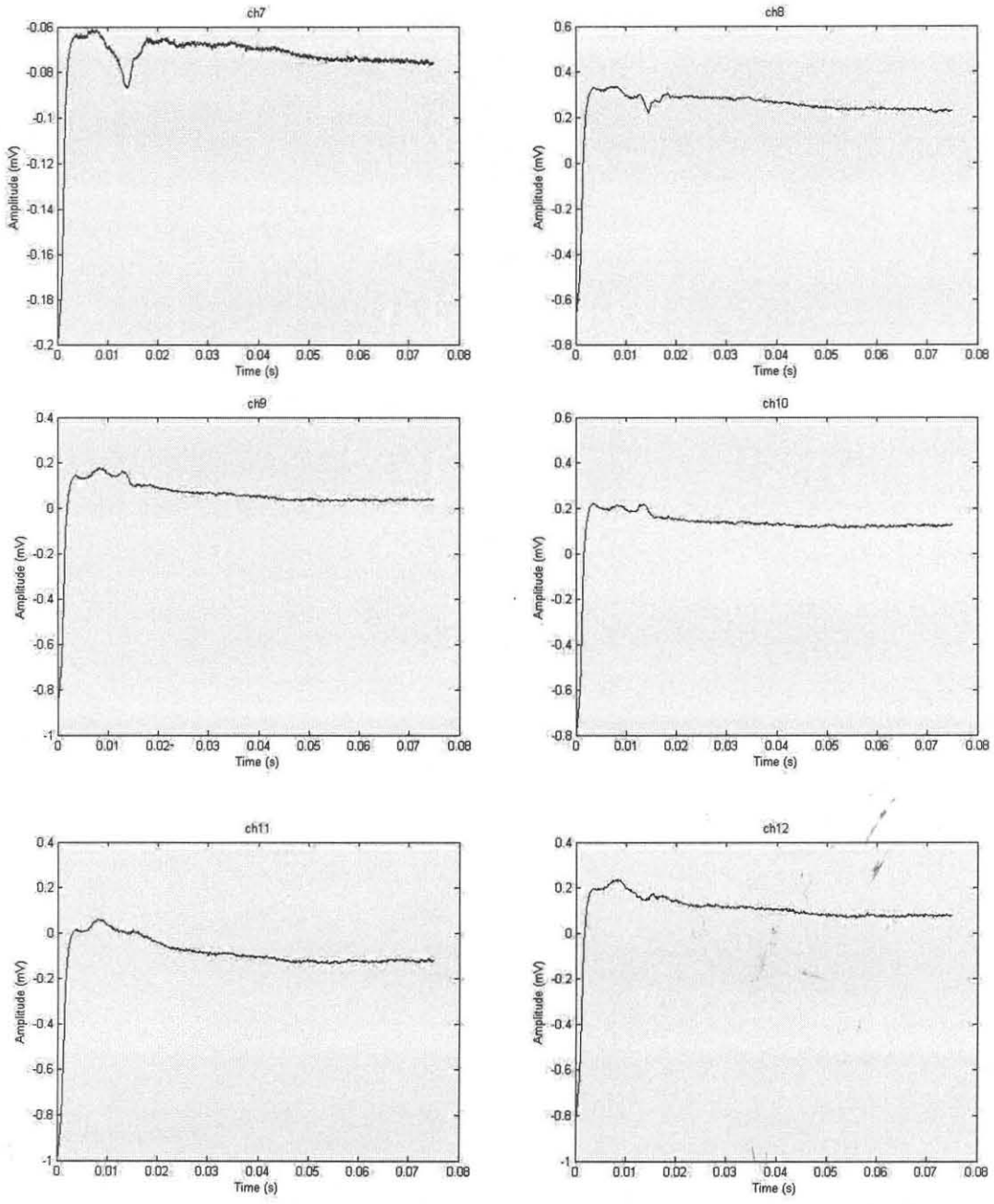

Figure 3.25 The spike triggered averaged field potentials for channels 7 though 12 evoked by stimulating the elbow region of the primary motor cortex.

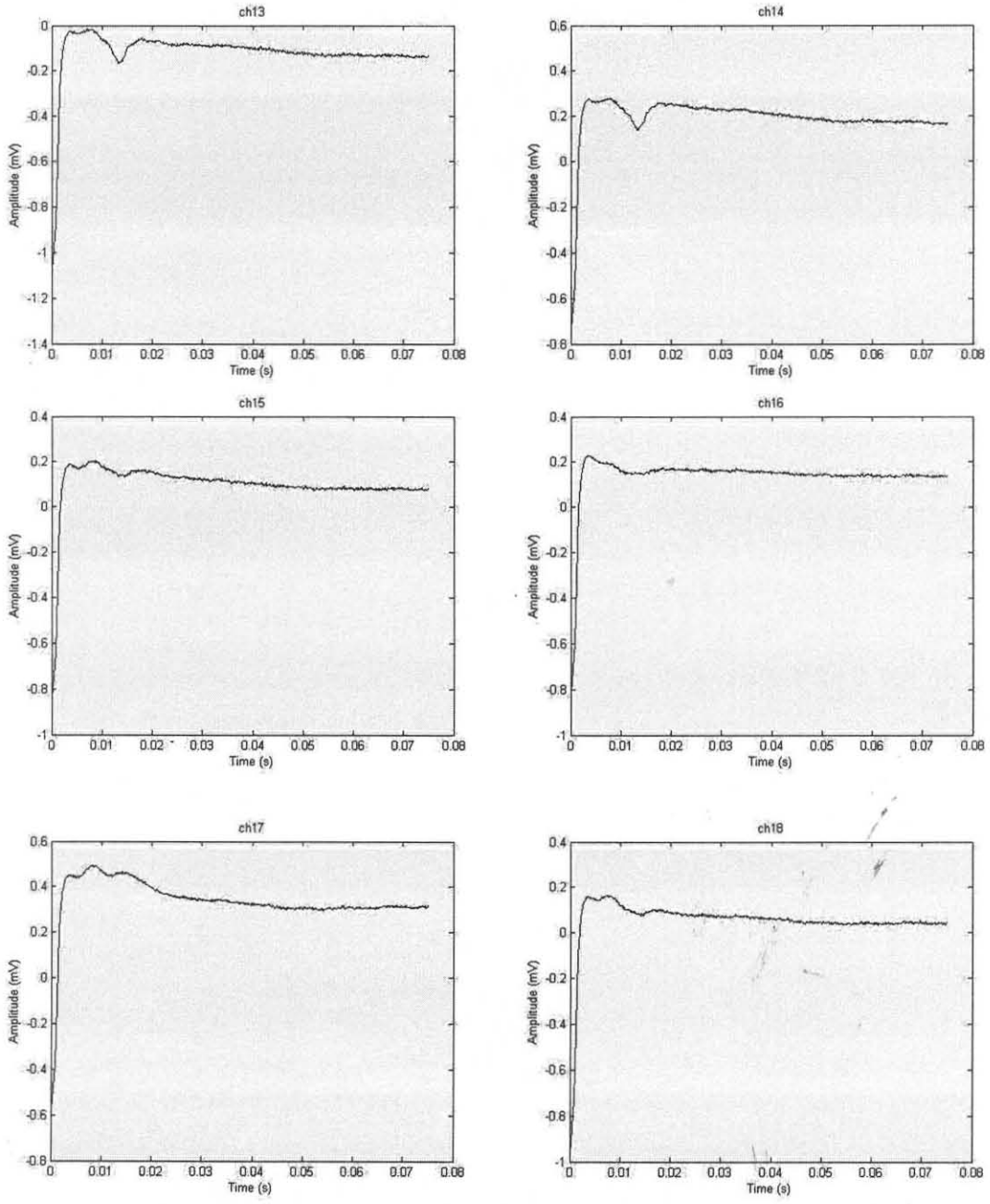

Figure 3.26 The spike triggered averaged field potentials for channels 13 though 18 evoked by stimulating the elbow region of the primary motor cortex.

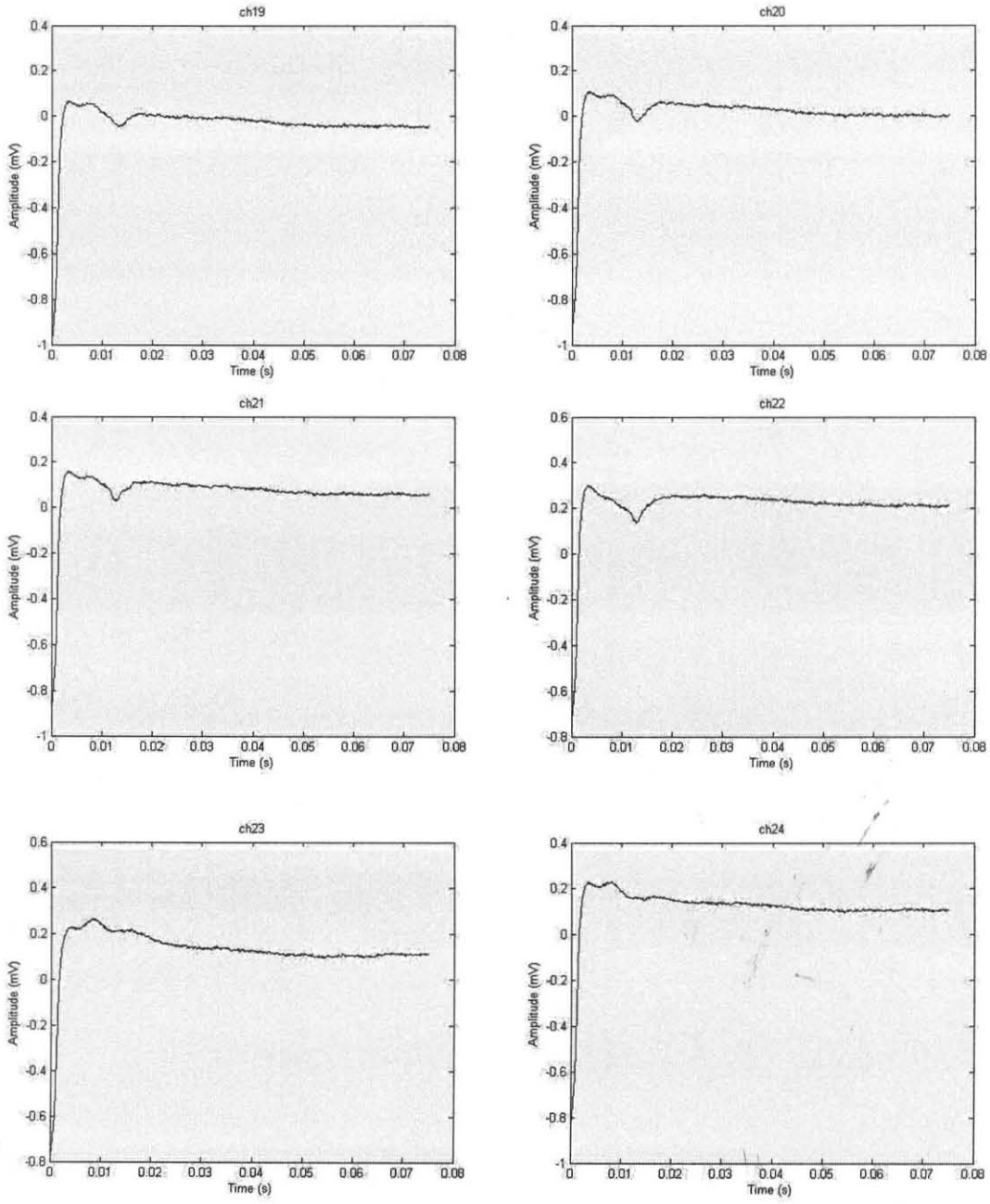

Figure 3.27 The spike triggered averaged field potentials for channels 19 though 24 evoked by stimulating the elbow region of the primary motor cortex.

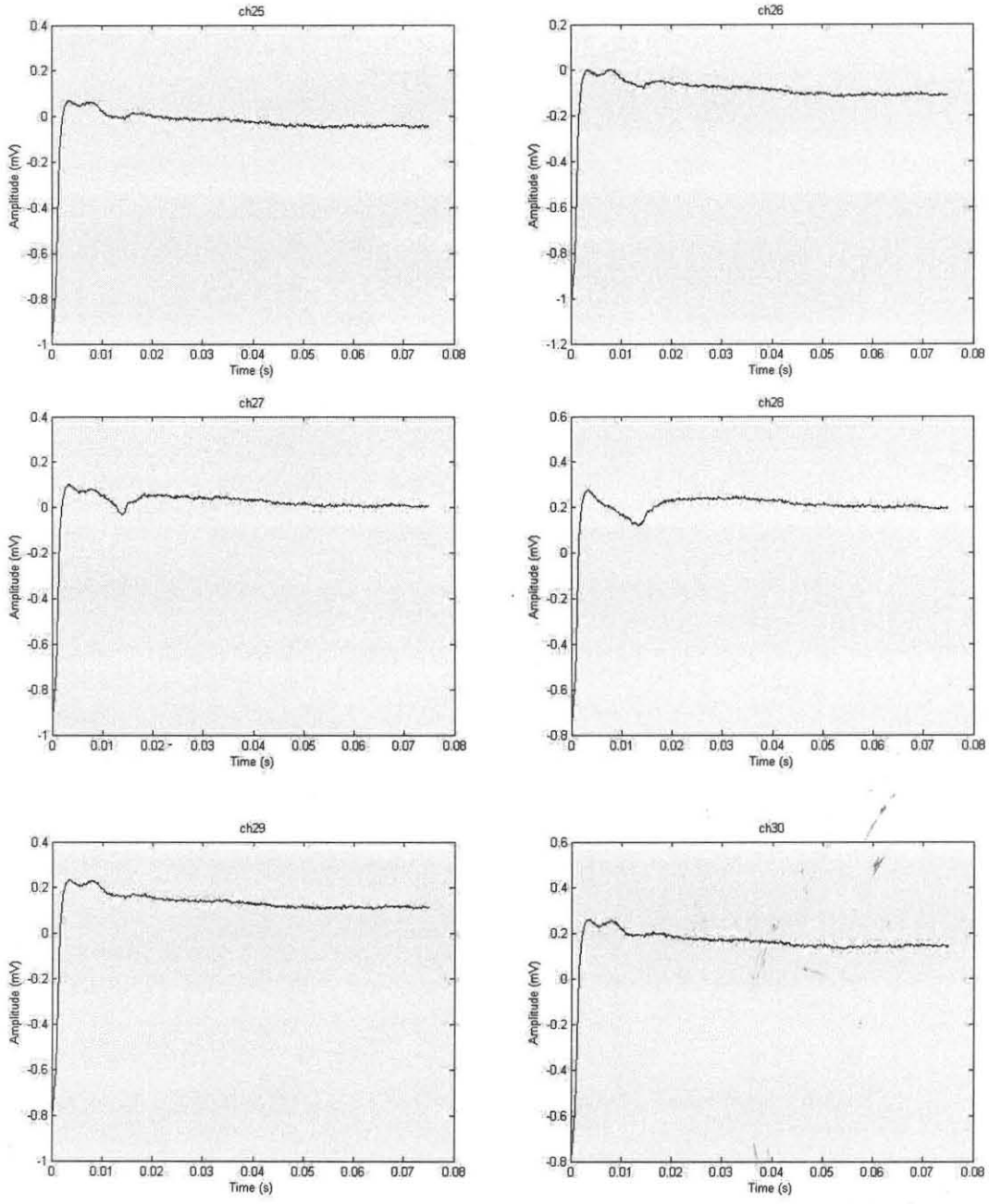

Figure 3.28 The spike triggered averaged field potentials for channels 25 though 30 evoked by stimulating the elbow region of the primary motor cortex.

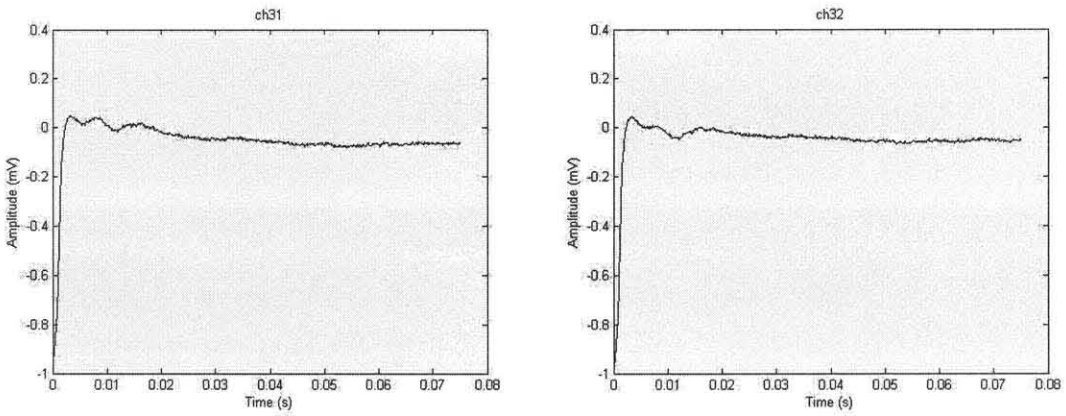

Figure 3.29 The spike triggered averaged field potentials for channels 29 though 32 evoked by stimulating the elbow region of the primary motor cortex.

The map of the elbow evoked potentials showed a region of activity in the rostro-lateral portion of the electrode array. The amplitudes of the averaged signals ranged from 0mV to 0.11V. The map of the amplitudes arranged to the electrode position is shown in Figure 3.30.

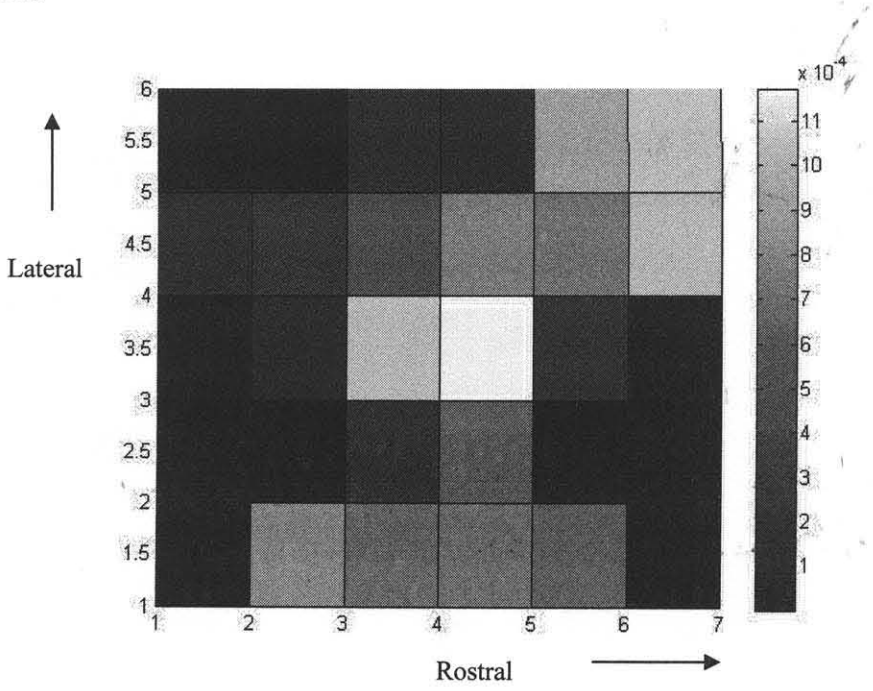

Figure 3.30 The amplitude maps of the elbow region evoked potentials, acquired from the spike triggered averaged signals, showing a region of activity in the rostro-lateral portion. The range of the amplitudes is from 0mV to 0.11mV.

First ten samples taken from the 22nd electrode position in the array are shown in Figure 3.31. These plots demonstrate that there was a large variation in the time of onset between each stimulation cycle. This variation was seen throughout the stimulation cycles. The 22nd electrode field potentials were chosen as a representative signal because they showed the best signal in the spike triggered averaging though the variation was seen in all electrode positions. The histogram in Figure 3.32 shows the distribution of the time of the N1 wave peak amplitude. The mean of the time of the N1 wave peak amplitude for the four was 15.7ms and the standard deviation was 1.7ms.

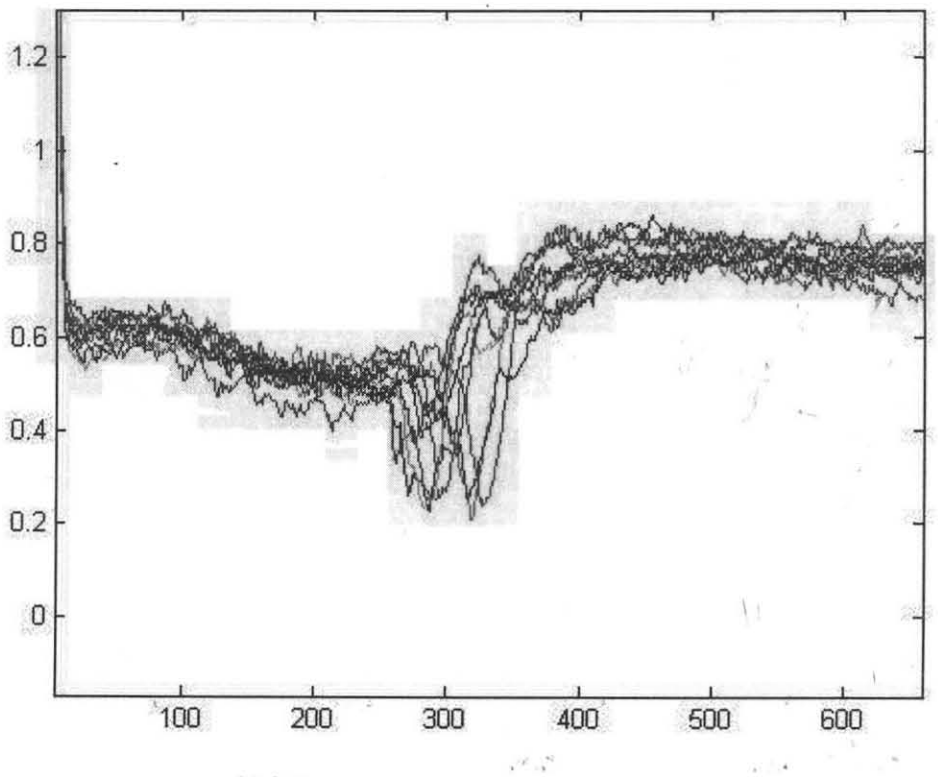

Figure 3.31 The evoked field potentials of first 10 samples recorded from the twenty second electrode position in the array for the stimulation of the elbow area of the primary motor cortex. The plots show that the time of onset was not steady from recording to recording as in the forearm and jaw recordings.

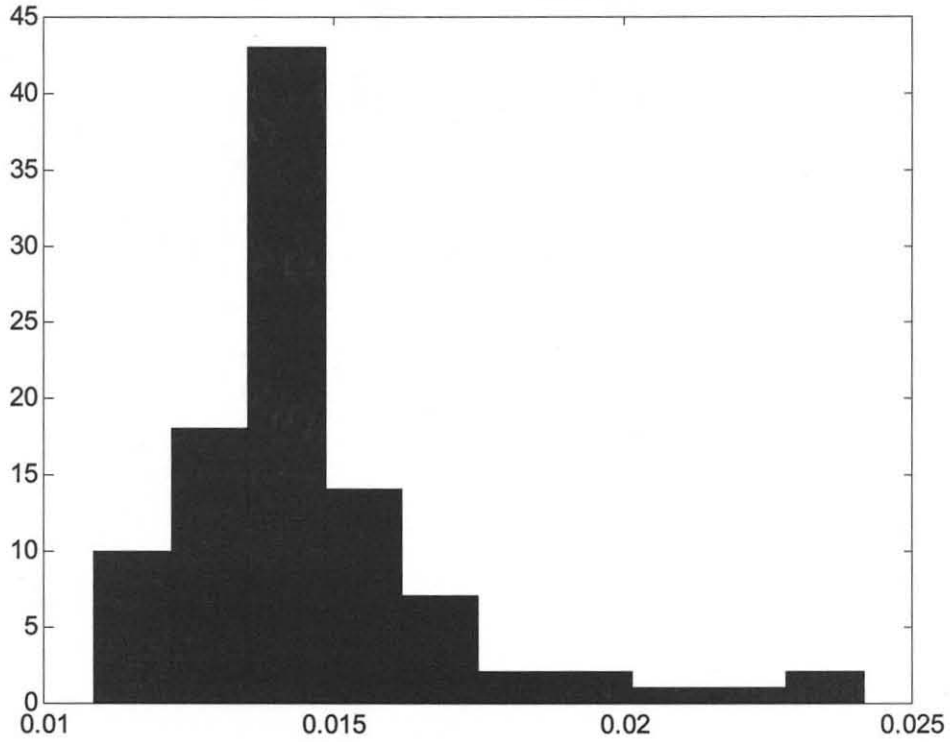

Figure 3.32 Histogram of the time of the N1 wave peak amplitude of the twenty second electrode position from the stimulation of the elbow area of the primary motor cortex for all 100 samples. The heights of the bars are the number of samples that are in each bin. The mean of the time of the N1 wave peak amplitude was 14.59ms and the standard deviation was 2.36ms.

3.2.4 Statistical Analysis

Figure 3.33 shows the normalized amplitude maps for the jaw, forearm only, and elbow area. The values were calculated by taking the minimum and maximum of the mossy fiber signal and were vectorally normalized. They show that the region of activity is generally maintained from the manually generated maps.

A)

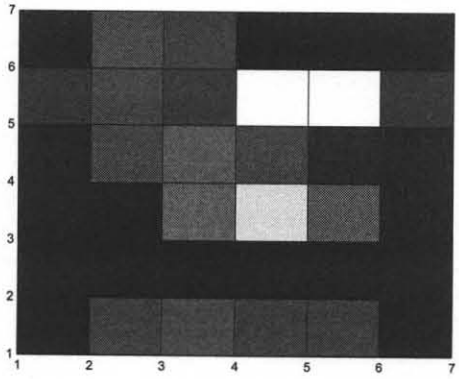

B)

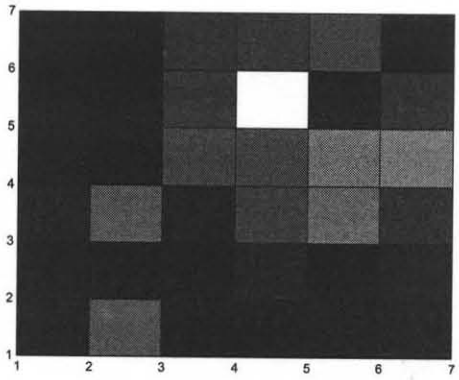

C)

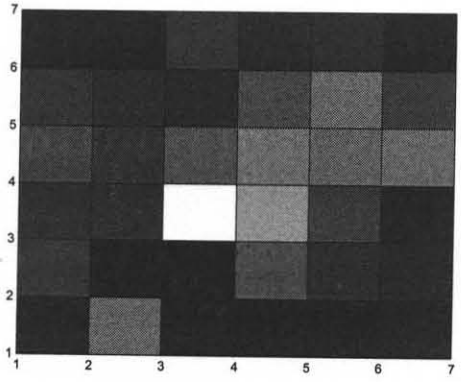

Figure 3.33 The normalized amplitude maps for the A) jaw area, B) forearm are, C) elbow area.

The normalized maps were compared using ANOVA analysis. The significant difference was determined with a p-value of 0.001. The results of the ANOVA analysis were mapped out to the same electrode pattern used in the amplitude maps. The black marks represent areas were the two maps were not significantly different and the white marks represent were they were significantly different.

Figure 3.34 shows the map of the comparison between the jaw region and the forearm only region. This comparison showed that 65.6% of the electrodes were significantly different. The map shows a black line the runs diagonally alone the middle of the graph representing the overlap of the signals in that region dividing the map into two regions for the two areas of stimulation.

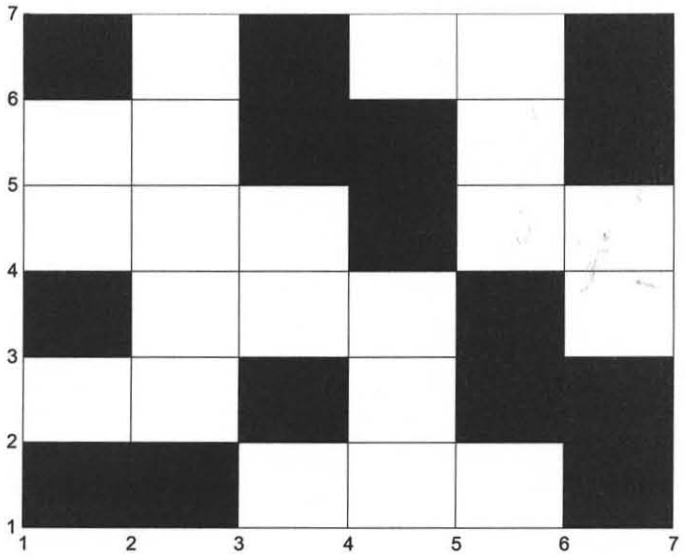

Figure 3.34 Map of the ANOVA results of the comparison of the jaw and forearm regions of activity. 65.6% of the electrodes electrode amplitudes were significantly different. The p-value was 0.001. The black squares represent electrodes were the amplitudes were not significantly different and the white marks represent were they were significantly different.

Figure 3.35 shows the map of the comparison between the forearm region and the elbow region. This comparison showed that 53.1% of the electrodes were significantly different. The map shows a black region in the upper right corner of the map that is consistent with the forearm region of activity showing a conservation of region of activity for different areas of forearm stimulation.

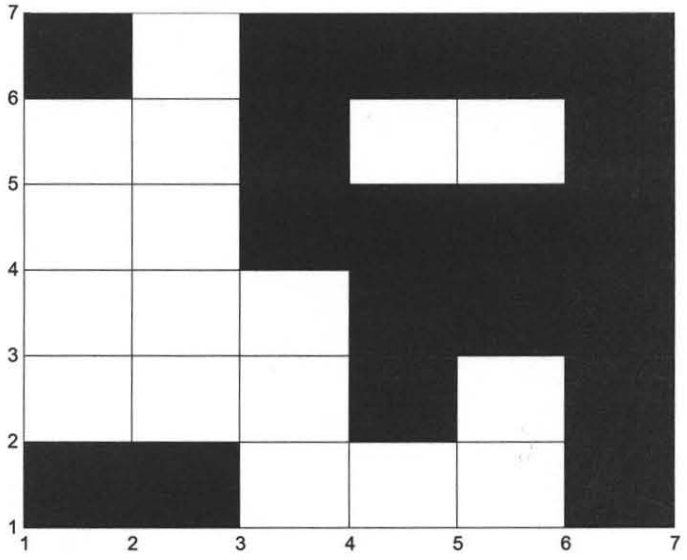

Figure 3.35 Map of the ANOVA results of the comparison of the forearm and elbow regions of activity. 53.1% of the electrodes electrode amplitudes were significantly different. The p-value was 0.001. The black squares represent electrodes were the amplitudes were not significantly different and the white marks represent were they were significantly different.

Figure 3.36 shows the map of the comparison between the jaw region and the elbow region. This comparison showed that 81.2% of the electrodes were significantly different. The map shows a slight black line that runs diagonally alone the middle of the graph representing the overlap of the signals in that region dividing the map into two regions for the two areas of stimulation in the motor cortex.

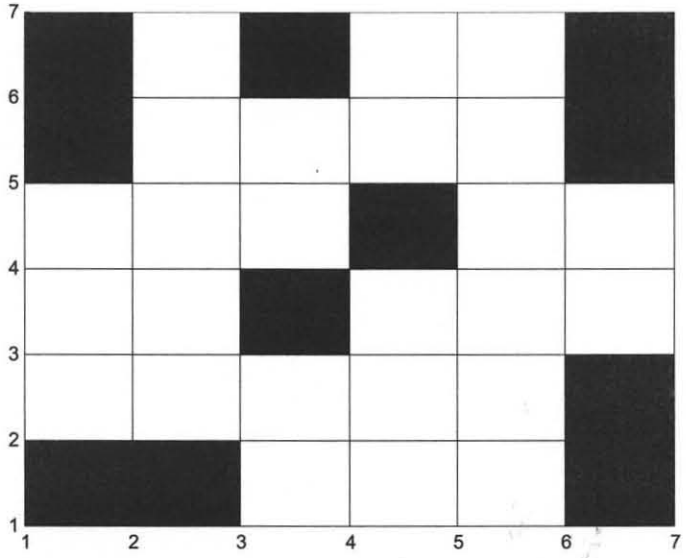

Figure 3.36 Map of the ANOVA results of the comparison of the jaw and elbow regions of activity. 81.2% of the electrodes electrode amplitudes were significantly different. The p-value was 0.001. The black squares represent electrodes were the amplitudes were not significantly different and the white marks represent were they were significantly different.

CHAPTER 4

DISCUSSION

4.1 Comparison of Peripherally Evoked Mossy Fiber Field Potentials to Previous Studies

The peripherally evoked mossy fiber field potentials (figure 4.1), had a signature consistent with that found by Eccles [18] and Armstrong [19]. The time of arrival for the N1 peak was averaged 2.27ms after the stimulation and the arrival time of the N3 peak averaged 4.34ms. This was very similar to the 2.4ms for the N1 peak and 5ms for the N3 peak found by Armstrong [19]. This demonstrated that the experimental setup used in these experiments was able to reproduce the results reported by other groups.

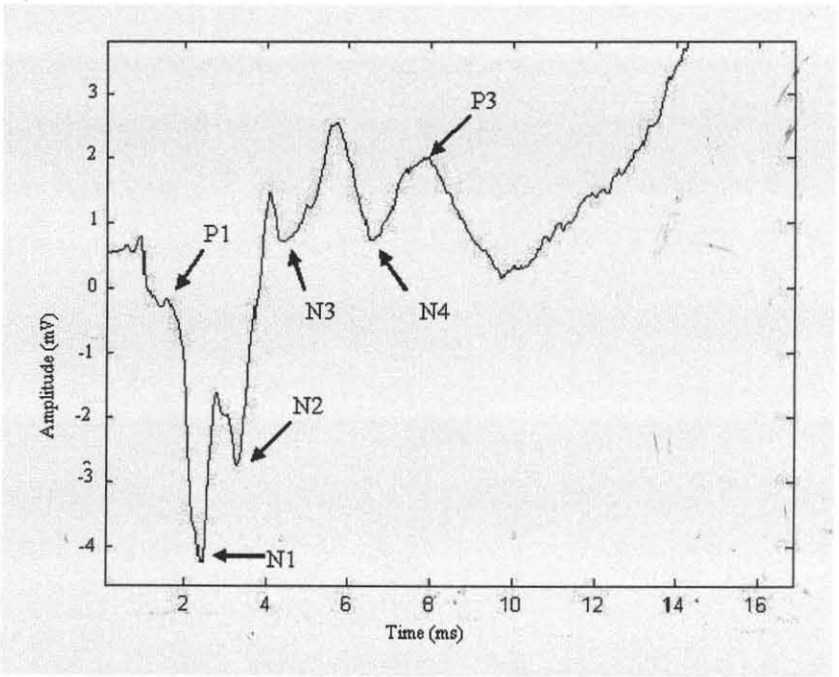

Figure 4.1 The peripherally evoked mossy fiber field potential recorded from the paramedian lobule of the cerebellar cortex. The average arrival time of the N1 peak was 2.27ms and the average arrival time of the N3 peak was 4.34ms.

4.2 Comparison of the Peripherally Evoked Signals to the Centrally Evoked Signals

The peripheral stimulation produced both a mossy fiber and a climbing fiber field potentials, however, the central stimulation produced only the mossy fiber field potential in the cerebellar cortex. The centrally evoked mossy fiber field potentials, Figure 4.2, showed all of the components seen in the peripherally evoked mossy fiber field potentials. The shape of the signal was also similar to that shown in the peripherally evoked mossy fiber field potentials. However the latency after the stimulation and time intervals between the compontents were longer in the centrally evoked potentials.

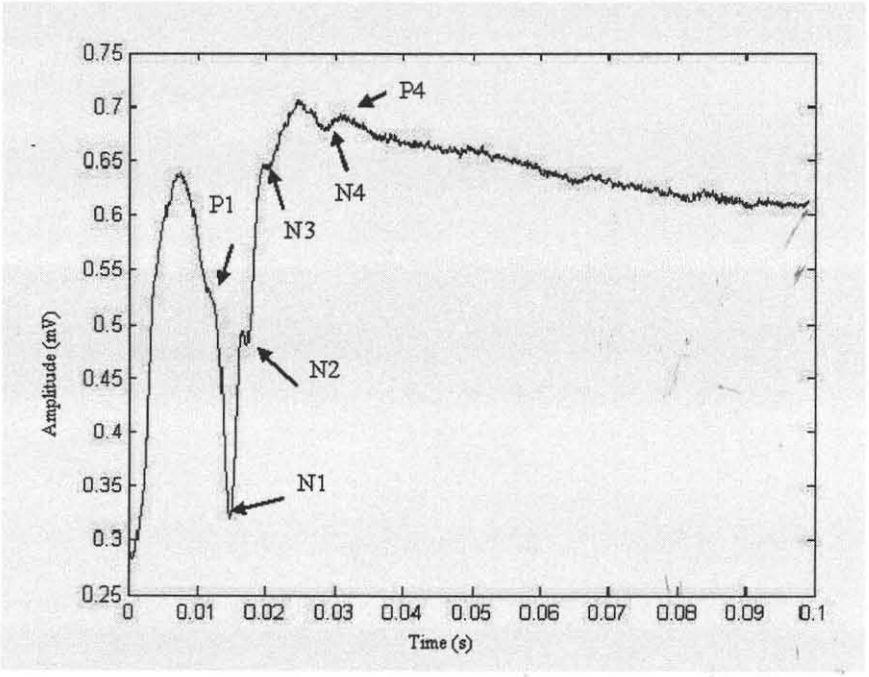

Figure 4.2 The centrally evoked mossy fiber field potential recorded from the parmedian cortex. The average time of the N1 peak was 13.81ms and the average time of the N3 peak was 20.29ms.

The N1 peak arived at 3.81ms following the stimulation for the centrally evoked potentials. The average arrival time of the N3 peak was 20.29ms. Compared to the peripherally evoked potentials, were the N1 peak arived at an average of 2.27ms and the N3 peak arrived at an average of 4.34ms, the centrally evoked potentials arrived an average of 11.54ms for the N1 peak and an average of 15.95ms later. The N1 occurred 6.84 ms earlier than the N3 peaks for the centrally evoked potentials. This was longer than the separation found in the peripherally evoked potentials with a difference of 2.07ms. The latency differences may be due to the differences in the path that the signals take to reach cerebellar cortex. The difference between the components may be due to the stimulation of interneurons in the motor cortex that would not be activated by the intramuscular stimulation used in the peripheral stimulation. The stimulation of the interneurons and the motorneurons may produce a weaker activation that was longer in duration so that it still was able pass through the synapses of the mossy fiber pathway however produced a longer wave for each component.

4.3 The Variation in Time of Onset between the Samples

The time delays by which various neural components occurred have varied substantially for the centrally evoked potentials. The standard deviation of the time of the N1 peak amplitude for the jaw recordings, which had the strongest amplitude of the three types tested, was 0.72ms. The standard deviation for the forearm only recordings, the next strongest amplitude, was 1.7ms. The standard deviation for the elbow recordings, the weakest amplitude of the three, was 2.36ms. The inverse relationship of the variation to the amplitude is most likely due to the decrease in signal to noise ratio.

4.4 Amplitude Maps

The comparison of the amplitude maps for the three stimulation sites shows unique patterns of activity for each stimulation site (Figure 4.3). The jaw stimulation produced the highest amplitude with a range varying from 2mV to 10mV. The forearm only stimulation produced the second highest amplitude with a range of 0.5mV to 4mV. The forearm and elbow stimulation produced the weakest stimulation with amplitudes up to 0.11mV. The jaw area stimulation produced an area of maximum activation in the middle of the recording area. Both the forearm only and the forearm and elbow areas showed a region of maximum activation in the rostro-lateral portion of the recording area. The maps show that there are distinct regions of activity for the jaw and forearm. The similarity between the forearm and elbow regions indicates there is a preservation of area of activation for stimulation of different sites in the forelimb area of the primary motor cortex.

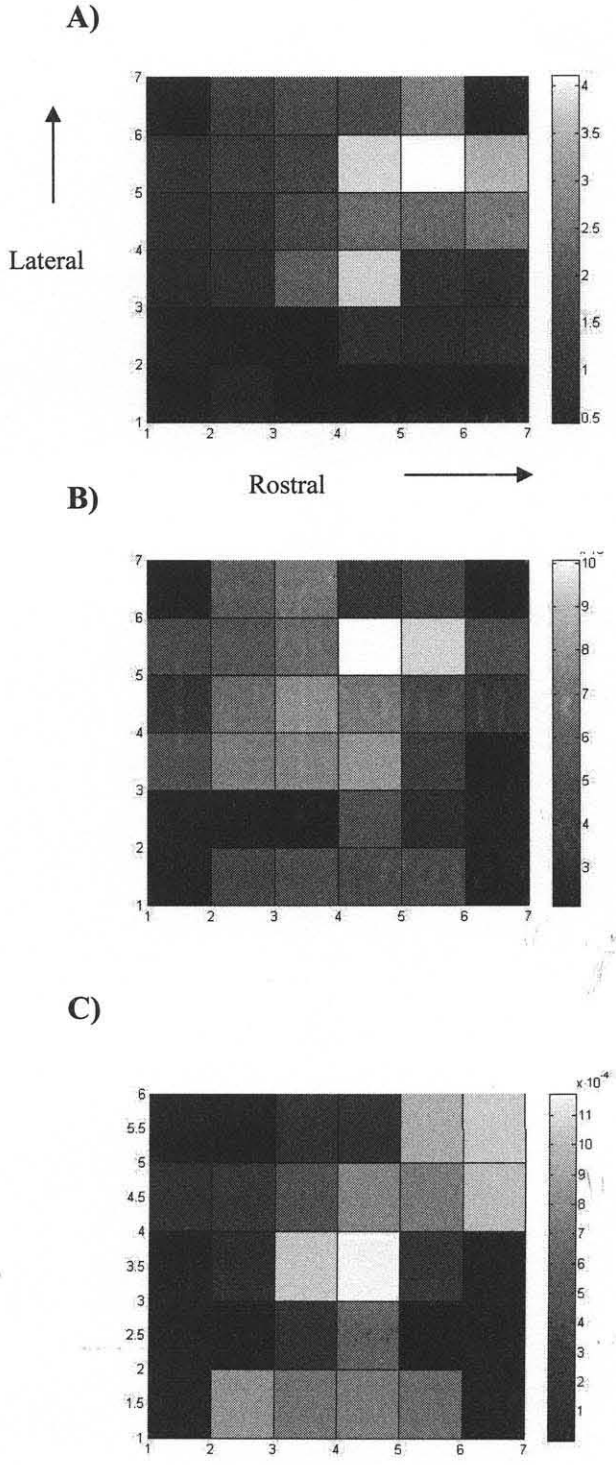

Figure 4.3 The amplitude maps of A) the forearm area stimulation, B) the jaw area stimulation, and C) the elbow area stimulation.

4.5 Statistical Analysis

The statistical analysis of the normalized amplitudes showed that there were areas for each activity that showed statistically significant difference. The comparison between the jaw and forearm only area showed 65.6% of the electrodes were significantly different. The comparison of the jaw and forearm and elbow regions showed 81.2% of the electrodes were significantly different. The comparison between the two forearm regions showed 53.1% of the electrodes were significantly different. This shows that different areas of stimulation produce unique maps of activity and that a large subset of electrodes can be used to distinguish between areas of activity.

CHAPTER 5

CONCLUSION

The peripheral data demonstrate that the FlexMEA microelectrode array is able to record the field potentials from the cerebellum consistent with penetrating electrodes and surface ball electrodes used in the past by other groups. The centrally evoked signals contained all of the components of the mossy fiber field potentials. The amplitude mapping showed all three central stimulation sites produced clearly demarked areas and that the 300μm pitch of the array was sufficient to obtain a detailed map to differentiate between various sites of activation in the motor cortex. The results demonstrate that the FlexMEA electrode and the experimental set up used in these experiments were able to record the field potentials from the cerebellar cortex and differentiate between the areas of activation for different sites of stimulation in the primary motor cortex. Study in more animals is needed to verify the results. Motivated by the preliminary results, the FlexMEA will be further explored with chronic implantations in behaving animals.

REFERENCES

1. Shepherd, G. M. Ed., *The Synaptic Organization of the Brain*. New York: Oxford Universiy Press, 2004.

2. Bosco, G. and Poppele, R. E., "Representation of multiple kinematic parameters of the cat hindlimb in spinocerebellar activity," *Journal of Neurophysiology*, vol. 78, pp. 1421-1432, 1997.

3. Casabona, A., Valle, M. S., Bosco, G., and Perciavalle, V., "Cerebellar encoding of limb position," *The Cerebellum*, vol. 3, pp. 172-177, 2004.

4. Johnson, M. T. V., and Ebner, T. J., "Processing of multiple kinematic signals in the cerebellum and motor cortices," *Brain Research Reviews*, vol. 33, pp. 155-168, 2000.

5. Fu, Q. G., Flament, D., Coltz, J. D., and Ebner, T. J., "Relationship of cerebellar Purkinje cell spike discharge to movement kinematics in the monkey," *Journal of Neurophysiology*, vol. 78, pp. 478-491, 1991.

6. Ebner, T. J., "A role for the cerebellum in the control of limb movement velocity," *Current Opinion in Neurobiology*, vol. 8, pp. 762-769, 1998.

7. Kawato, M., and Gomi, H., "A computational model of four regions of the cerebellum based on feedback-error learning," *Biological Cybernetics*, vol. 68, pp. 95-103, 1992.

8. Kettner, R. E., et al., "Prediction of complex two-dimensional trajectories by a cerebellar model of smooth pursuit eye movement," *Journal of Neurophysiology*, vol. 22, pp. 2115-2130, 1997.

9. Hirano, T., "Motor control mechanism by the cerebellum," *The Cerebellum*, vol. 5, pp. 296-300, 2006.

10. Nowak, D. A., Topka, H., Timmann, D., Boecker, H., and Hermsdorfer, J., "The role of the cerebellum for predictive control of grasping," *The Cerebellum*, vol. 6, pp. 7-17, 2007.

11. Kawato, M., "Inverse dynamics models in the cerebellum," *in International Joint Confernce on Neural Networks*, pp.1329-1335, 1993.

12. Shadmehr, R., and Krakauer, J. W., "A computational neuroanatomy for motor control," *Experimental Brain Research*, vol. 185, pp. 359-381, 2008.

13. Manto, M., and Bastian, A. J., "Cerebellum and the deciphering of motor coding," *The Cerebellum*, vol. 6, pp. 3-6, 2007.

14. Kandel, E. R., Shwartz, J. H., Jessell, T. M., *Principles of Neural Science*, New York: McGraw-Hill, 2000.

15. Enger, M., and Brodal, P., "Organization of corticopontocerebellar connections to the paramedian lobule in the cat," *Anatomy and Embryology*, vol. 172, pp. 227-238, 1985.

16. Atkins, M. J., and Apps, R., "Somatotopical organization within the climbing fibre projection to the paramedian lobule and copula pyramidis of the rat cerebellum," *The Journal of Comparative Neurology*, vol. 389, pp. 249-263, 1997.

17. Odeh, F., Ackerley, R., Bjaalie, J. G., and Apps, R., "Pontine maps linking somatosensory and cerebellar cortices are in register with climbing fiber somatopy," *The Journal of Neuroscience*, vol. 25, pp. 5680-5690, 2005.

18. Eccles, J. C., Sasaki, K., and Strata, P., "Interpretation of the potential fields generated in the cerebellar cortex by a mossy fiber volley," Experimental *Brain Research*, vol. 3, pp. 58-80, 1967.

19. Armstrong, D. M., Drew, T., "Responses in the posterior lobe of the rat cerebellum to electrical stimulation of cutaneous afferents to the snout," *Journal of Physiology*, vol. 309, pp. 357-374, 1980.